SECOND COSMOLOGY SCHOOL

Ministry of Science and Higher Education
Republic of Poland

INTRODUCTION TO COSMOLOGY
Kielce, Poland 11.07 - 24.07.2016

HECOLS
Polish-French collaboration in astrophysics

CAMK PAN

Naukaonline.pl ACADEMIA

Cosmology with strong lensing systems

Marek Biesiada

UNIVERSITY OF SILESIA IN KATOWICE

Instytut Fizyki im. Augusta Chełkowskiego

Department of Astrophysics and Cosmology
Institute of Physics,
University of Silesia
Katowice, Poland

Gravitational lenses

Why?

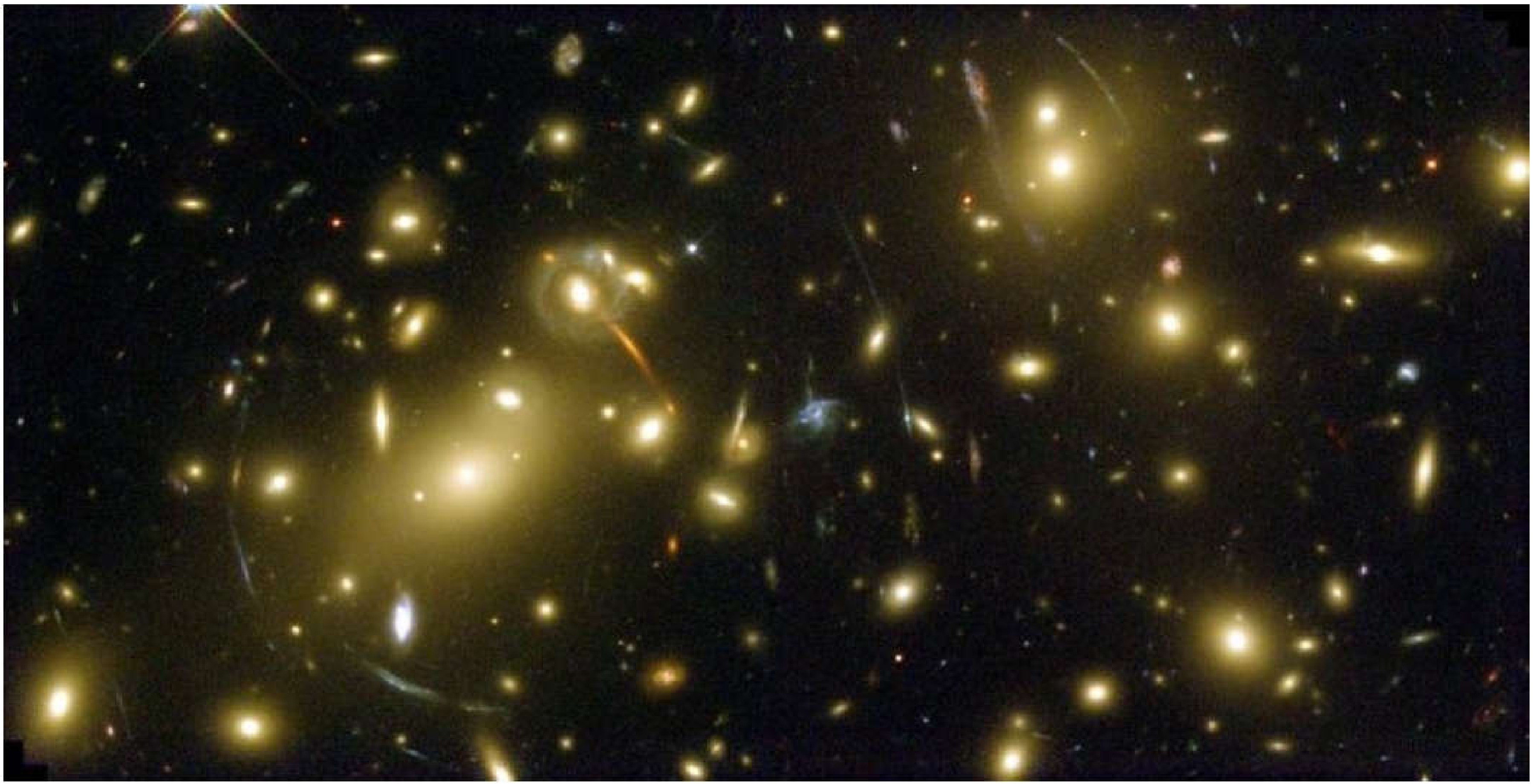

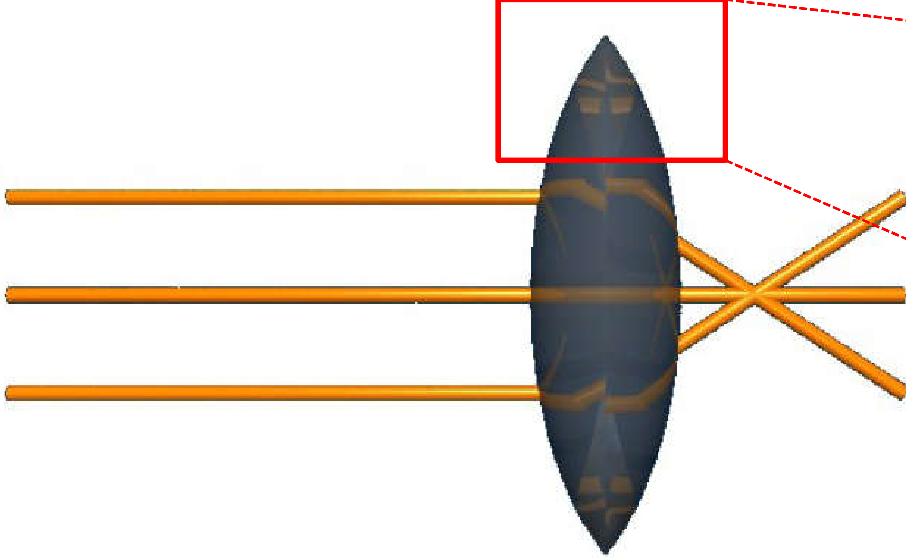

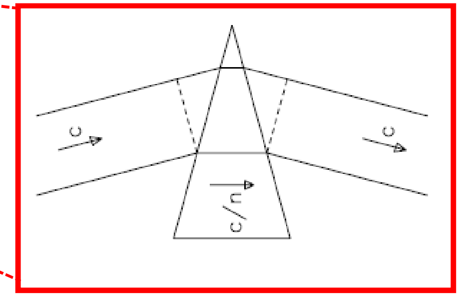

Usual lens bends light because of the difference in the index of refraction **n**

But in vacuum
n = 1 !

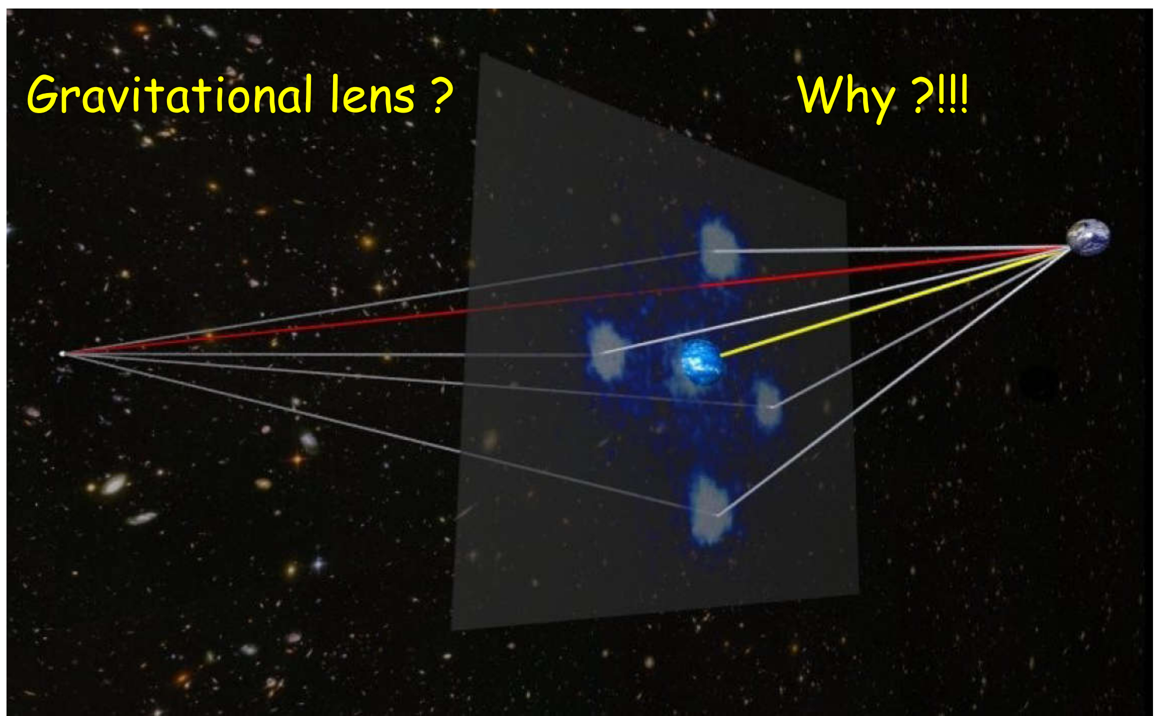

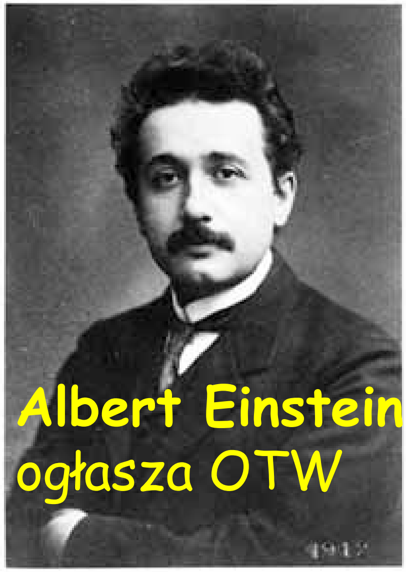

It all began in 1915

2015 –Centenary of GR

United Nations Educational, Scientific and Cultural Organization

International Year of Light 2015

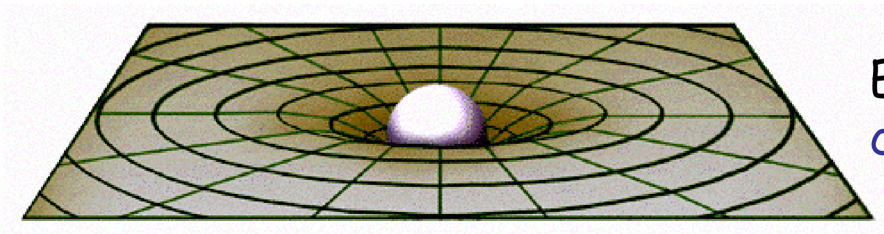

Free motion in curved spacetime
is along geodesics
(the shortest paths)

Einstein Equations – matter curves spacetime

$$G_{\mu\nu} = \frac{8\pi G}{c^4} T_{\mu\nu}$$

Bending of light near the surface of the Sun

Curvature of spacetime
affects not only trajectories of massive bodies, but
also of the light !

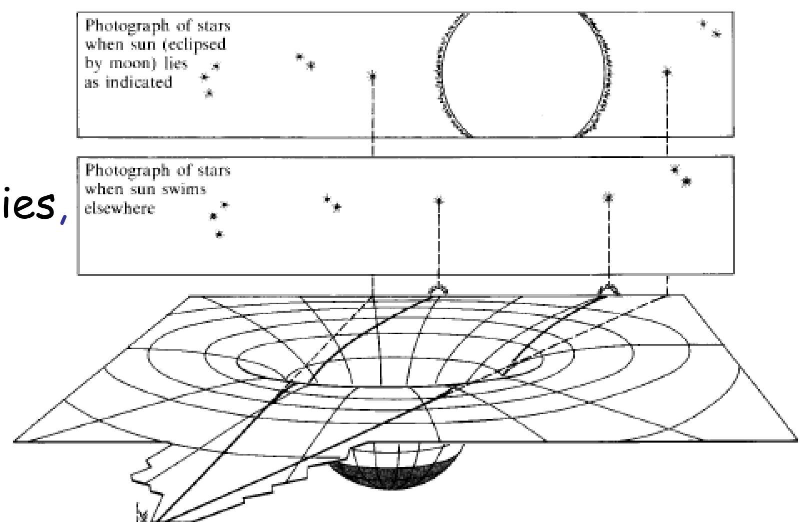

Bending of light - History:

John Michell (1724-1793) in a letter to
Henry Cavendish (1731-1810) [independently von Soldner 1801]

•suppose that light is comprised of particles

• in the gravitational field of the Sun light particle moves along a trajectory (being a solution of a Newtonian 2 body problem)

• in general it would be a conical section (elipse, parabola, hyperbola)

• for light it's clearly a hyperbola ($c \gg V_{esc}$)

•hence the bending angle $$\alpha = \frac{2GM}{c^2 b}$$

• for a corpuscule of light grazing the Sun

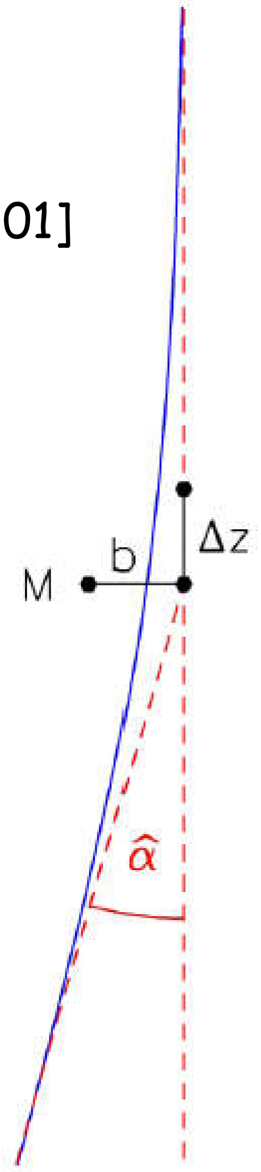

$$m = M_\odot = 1.989 \times 10^{30}\mathrm{kg}$$
$$R = R_\odot = 6.96 \times 10^{8}\mathrm{m}$$

$$\alpha = \frac{2GM}{c^2 R} = 0''.875$$

„seeing" 0."5 – 1."

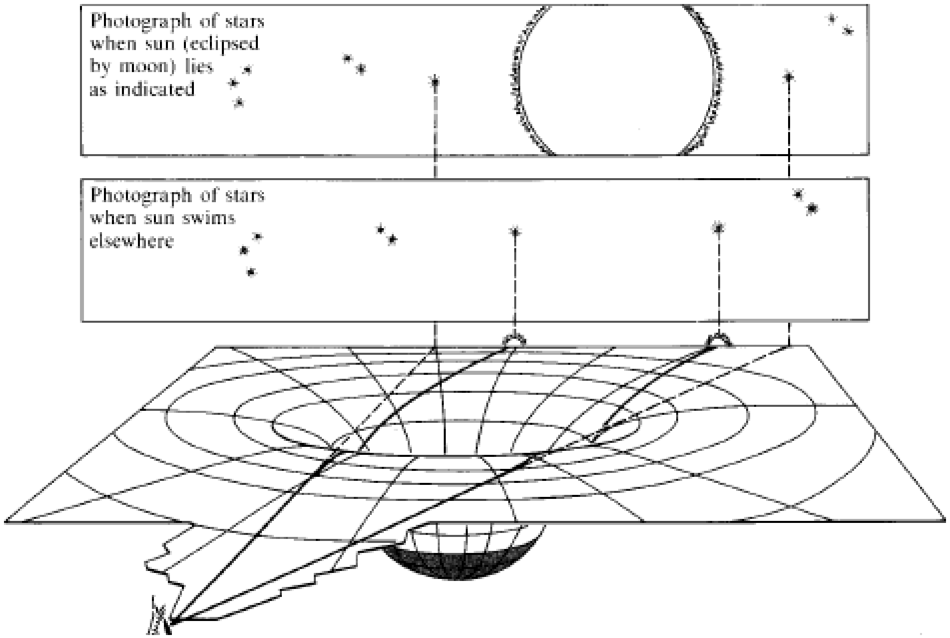

Light bending near
the surface of the Sun

Calculations
within
the GR

$$\alpha = \frac{4GM}{c^2 R} = 1''.75$$

Einstein becomes a „celebrity" – within next year more than 100 books on Relativity Theory are written

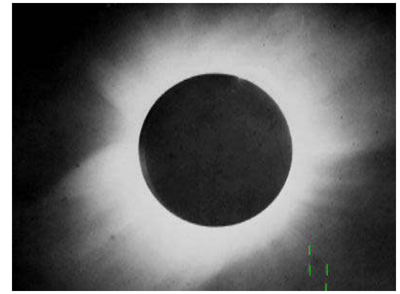

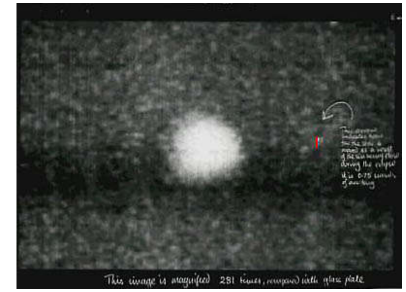

29.V.1919
Sir Arthur Eddington

Total solar eclipse
in front of the
Hyad cluster

Gravitational Lensing

Spherically symmetric lens model – the simplest realistic case

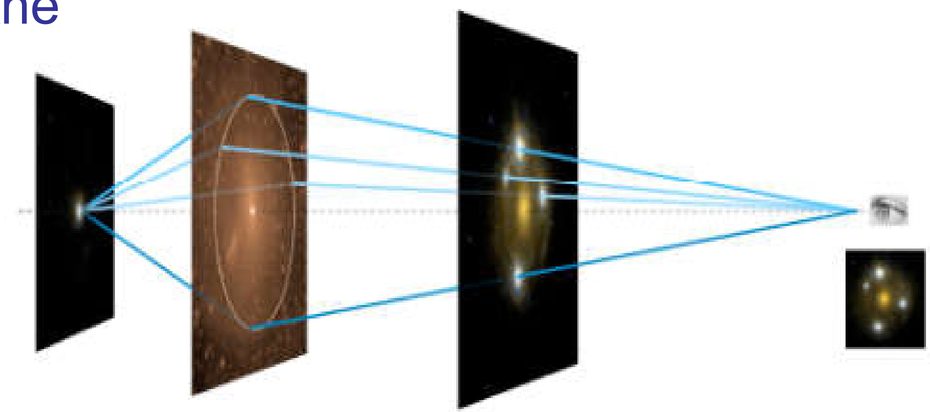

Einstein radius (determined by **mass** !)
- defines **characteristic angular scale**

$$\vartheta_E = \sqrt{\frac{4GM_E}{c^2}\frac{D_{ls}}{D_s D_l}}$$

Two images form on the opposite side of the lens

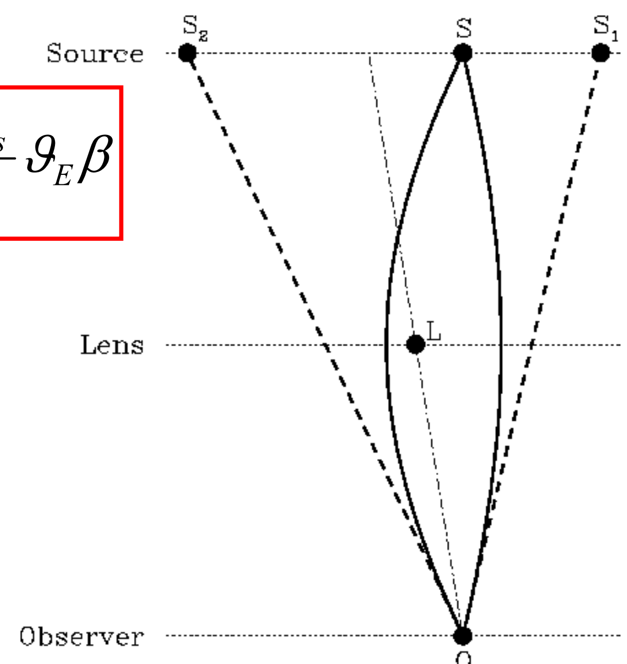

Time delay between images

$$\Delta t = \frac{2(1+z_l)}{c}\frac{D_l D_s}{D_{ls}}\vartheta_E \beta$$

Two lensing regimes:

Strong:
- multiple images
- time delays between images – (a method to measure H_0)

Weak: image distortion

Gravitational lensing – early days

• Einstein skeptical concerning this effect

solar mass 1 $M_\odot$ lenses, with distances 5 – 10 kpc typical for the Galaxy
have Einstein rings 0".001 – **unobservable !**

•Zwicky 1937 (!) galaxies as lenses

masses 10^{11} – 10^{12} $M_\odot$
distances 10 Mpc – 1 Gpc
Einsteina ring **1".**

This is observable !

Gravitational microlensing

LENS-LIKE ACTION OF A STAR BY THE DEVIATION OF LIGHT IN THE GRAVITATIONAL FIELD

SOME time ago, R. W. Mandl paid me a visit and asked me to publish the results of a little calculation, which I had made at his request. This note complies with his wish.

The light coming from a star A traverses the gravitational field of another star B, whose radius is R_o. Let there be an observer at a distance D from B and at a distance x, small compared with D, from the extended central line $\overline{AB}$. According to the general theory of relativity, let α_o be the deviation of the light ray passing the star B at a distance R_o from its center.

For the sake of simplicity, let us assume that $\overline{AB}$ is large, compared with the distance D of the observer from the deviating star B. We also neglect the eclipse (geometrical obscuration) by the star B, which indeed is negligible in all practically important cases. To permit this, D has to be very large compared to the radius R_o of the deviating star.

It follows from the law of deviation that an observer situated exactly on the extension of the central line $\overline{AB}$ will perceive, instead of a point-like star A, a luminius circle of the angular radius β around the center of B, where

$$\beta = \sqrt{\alpha_o \frac{R_o}{D}}.$$

It should be noted that this angular diameter β does not decrease like $1/D$, but like $1/\sqrt{D}$, as the distance D increases.

Of course, there is no hope of observing this phenomenon directly. First, we shall scarcely ever approach closely enough to such a central line. Second, the angle β will defy the resolving power of our instruments. For, α_o being of the order of magnitude of one second of arc, the angle R_o/D, under which the deviating star B is seen, is much smaller. Therefore, the light coming from the luminous circle can not be distinguished by an observer as geometrically different from that coming from the star B, but simply will manifest itself as increased apparent brightness of B.

The same will happen, if the observer is situated at a small distance x from the extended central line $\overline{AB}$. But then the observer will see A as two point-like light-sources, which are deviated from the true geometrical position of A by the angle β, approximately.

The apparent brightness of A will be increased by the lens-like action of the gravitational field of B in the ratio q. This q will be considerably larger than unity only if x is so small that the observed positions of A and B coincide, within the resolving power of our instruments. Simple geometric considerations lead to the expression

$$q = \frac{l}{x} \cdot \frac{1 + \frac{x^2}{2l^2}}{\sqrt{1 + \frac{x^2}{4l^2}}},$$

where

$$l = \sqrt{\alpha_o D R_o}.$$

If we are interested mainly in the case $q \gg 1$, the formula

$$q = \frac{l}{x}$$

is a sufficient approximation, since $\frac{x^2}{l^2}$ may be neglected.

Even in the most favorable cases the length l is only a few light-seconds, and x must be small compared with this, if an appreciable increase of the apparent brightness of A is to be produced by the lens-like action of B.

Therefore, there is no great chance of observing this phenomenon, even if dazzling by the light of the much nearer star B is disregarded. This apparent amplification of q by the lens-like action of the star B is a most curious effect, not so much for its becoming infinite, with x vanishing, but since with increasing distance D of the observer not only does it not decrease, but even increases proportionally to $\sqrt{D}$.

ALBERT EINSTEIN

INSTITUTE FOR ADVANCED STUDY,
PRINCETON, N. J.

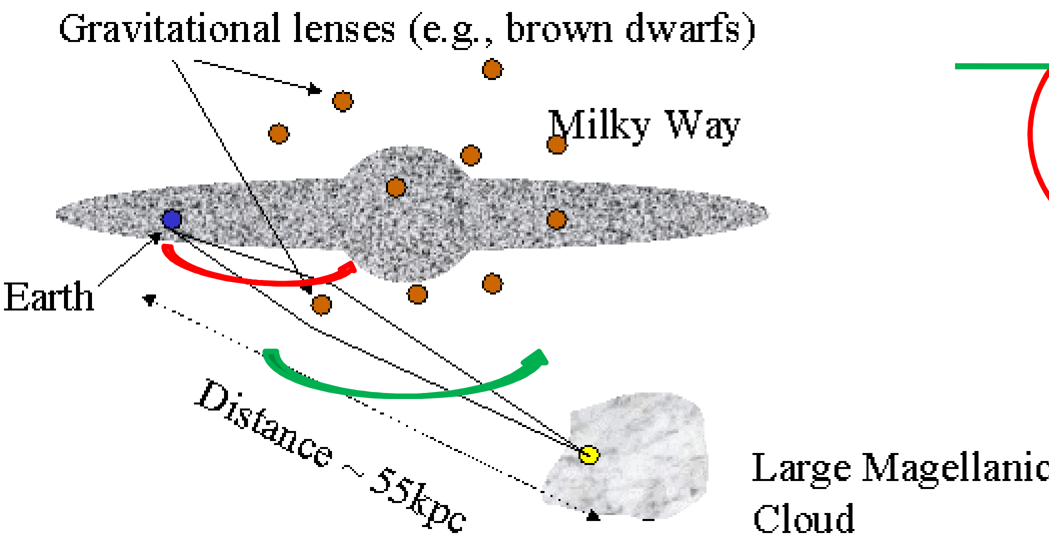

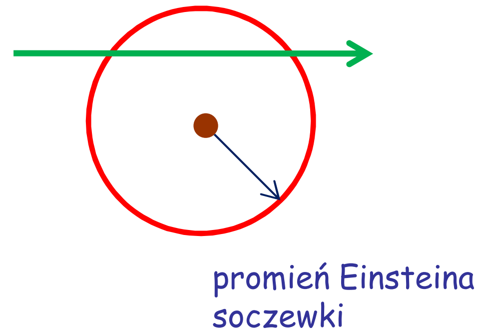

relative motion source vs. lens

Bohdan Paczyński 1986

observational idea of microlensing

When source crosses
the Einstein ring 2 images appear
* separated by ca. 1 mas
* no way to see them resolved
* we see 1 image of the source
but brighter than without lensing
* relative motion of the source
w.r.t. lens leads to variable
brightness of the source

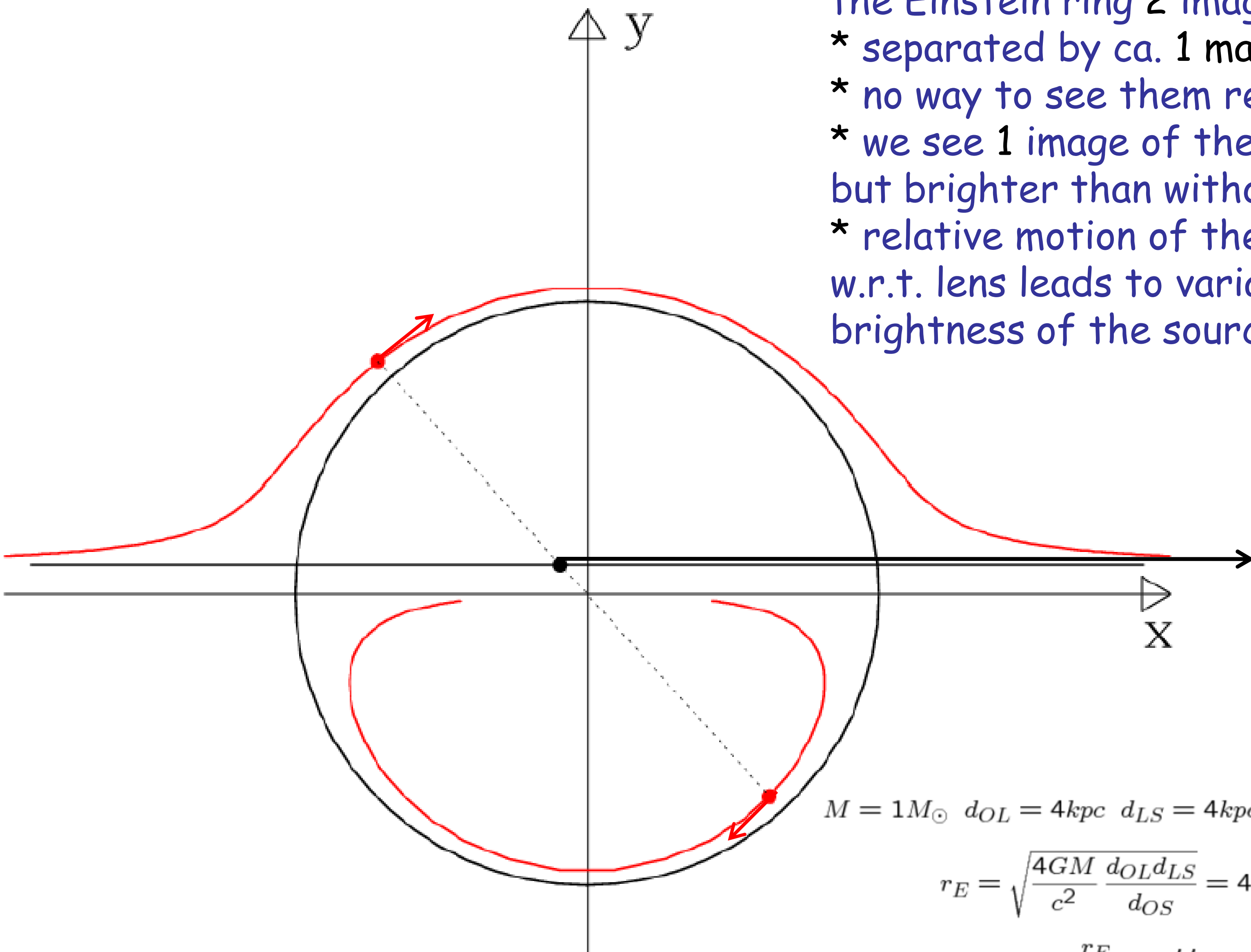

$M = 1 M_\odot \;\; d_{OL} = 4kpc \;\; d_{LS} = 4kpc \;\; d_{OS} = 8kpc$

$$r_E = \sqrt{\frac{4GM}{c^2} \frac{d_{OL} d_{LS}}{d_{OS}}} = 4AU$$

$$\Theta_E = \frac{r_E}{d_{OL}} = 0'.'001$$

Microlensing lightcurve

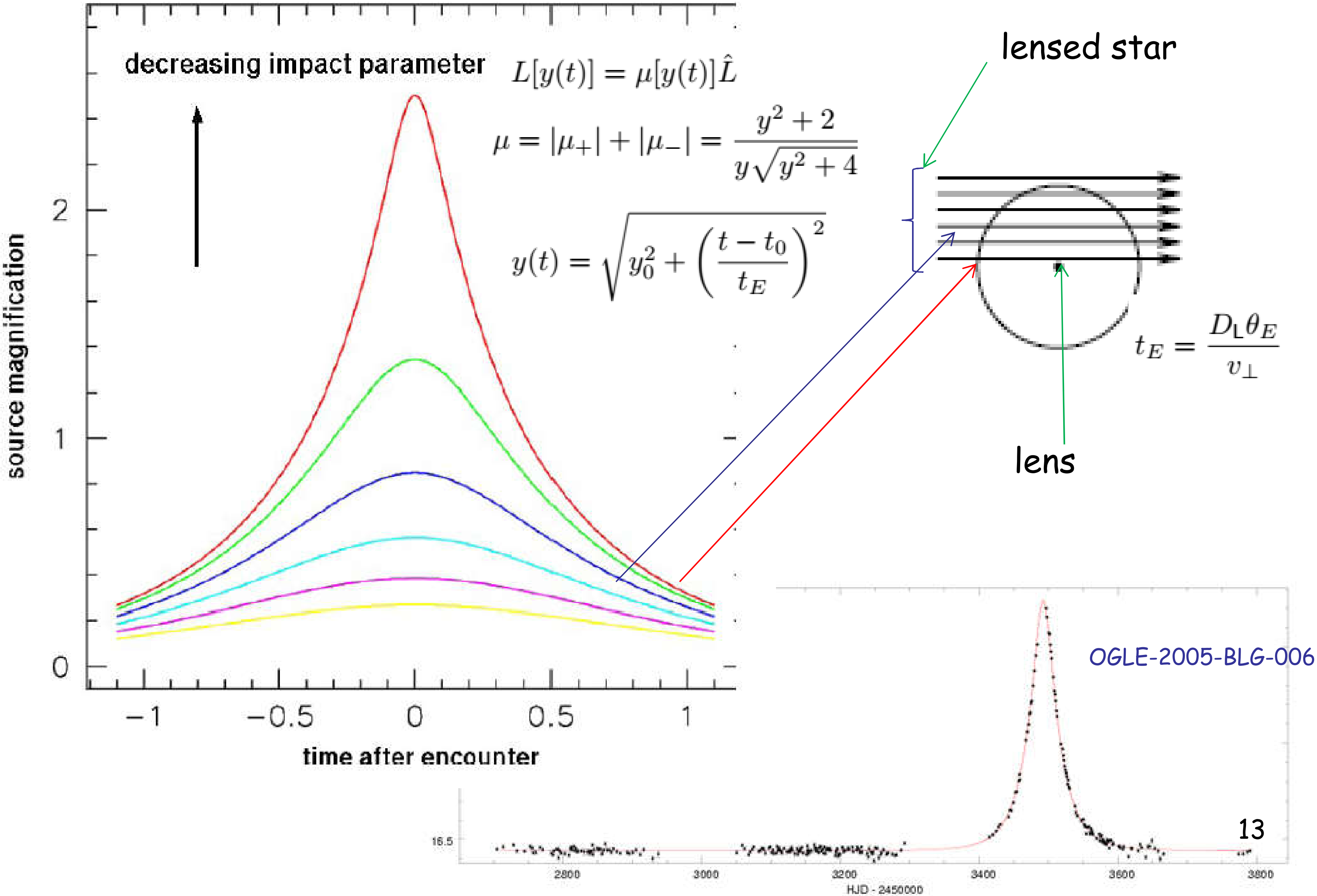

$$L[y(t)] = \mu[y(t)]\hat{L}$$

$$\mu = |\mu_+| + |\mu_-| = \frac{y^2+2}{y\sqrt{y^2+4}}$$

$$y(t) = \sqrt{y_0^2 + \left(\frac{t-t_0}{t_E}\right)^2}$$

$$t_E = \frac{D_L \theta_E}{v_\perp}$$

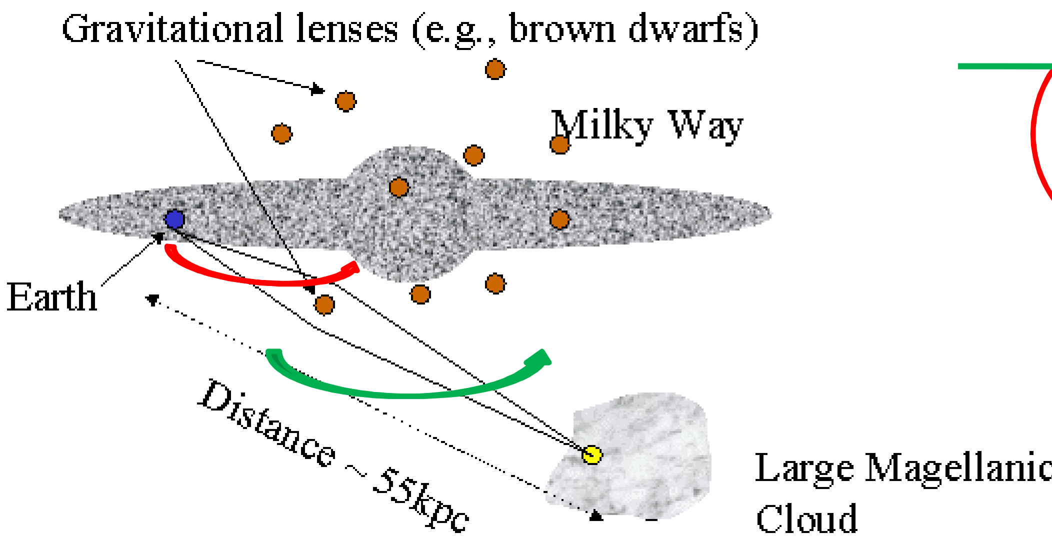

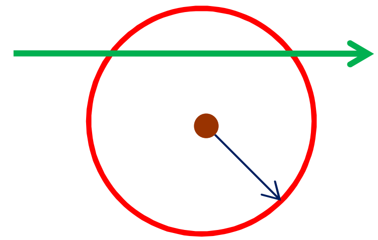

Bohdan Paczyński 1986

observational idea of microlensing

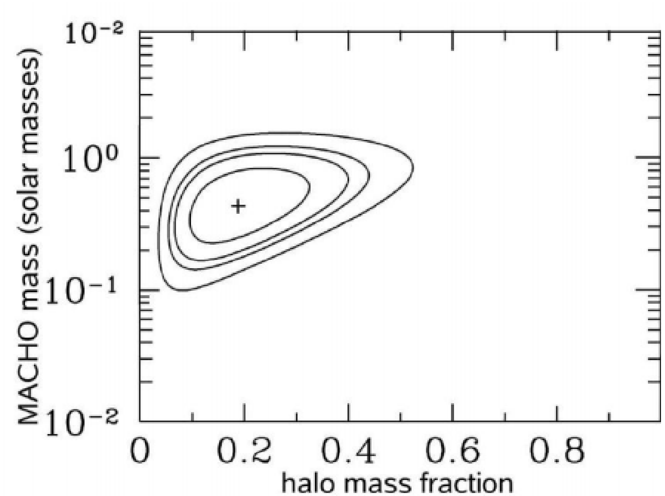

$$\tau_{\mathrm{LMC(MACHO)}} = 1.2^{+0.4}_{-0.3} \times 10^{-7}$$

Alcock C. et al. (2000) ApJ 542, 281

$$\tau_{\mathrm{LMC(EROS)}} \approx 10^{-7}$$

Afonso C. et al. (2003) A&A 400, 951

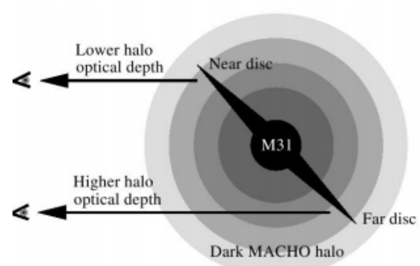

Pixelensing towards M31

Kerins E. et al. (2001) MNRAS 323, 13

Search for extraterrestial planets – B.Paczyński, S. Mao 1991

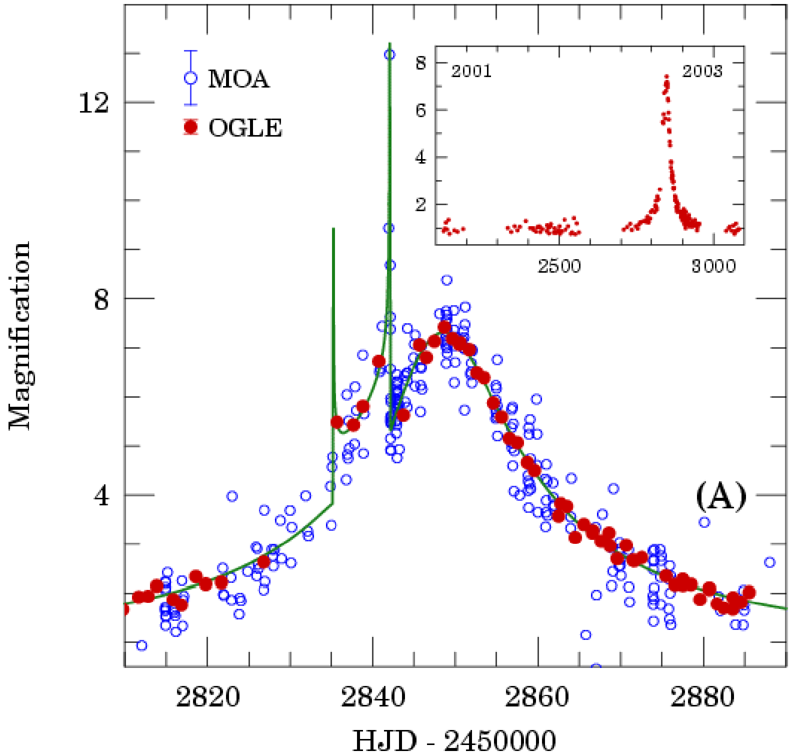

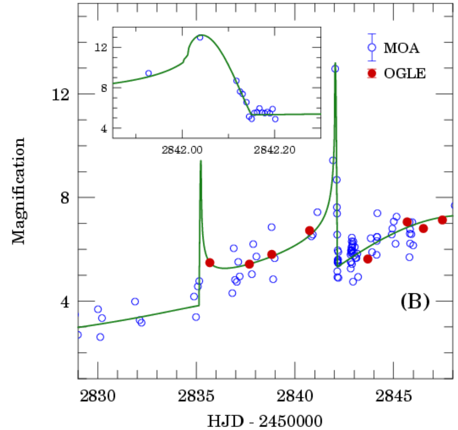

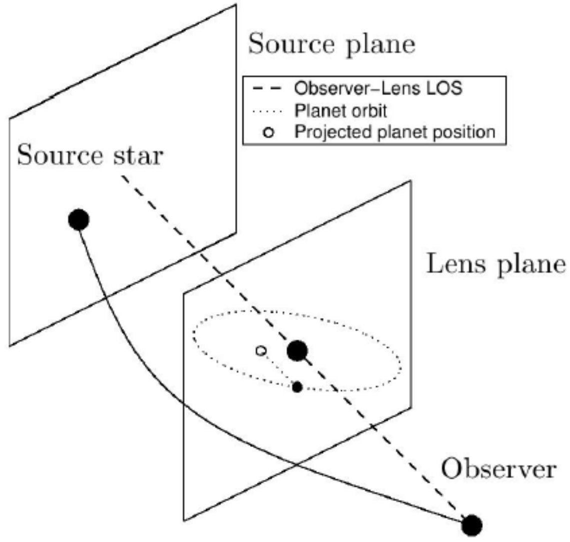

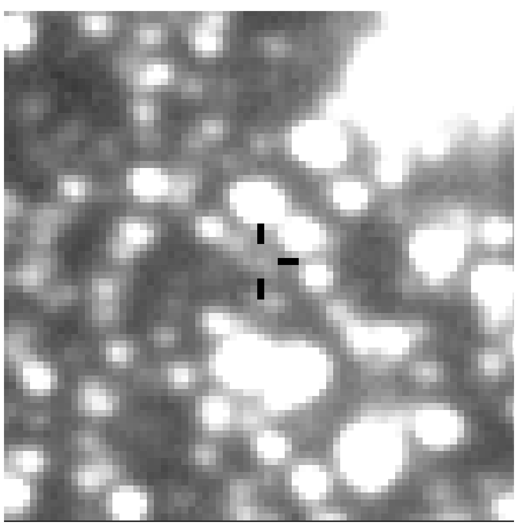

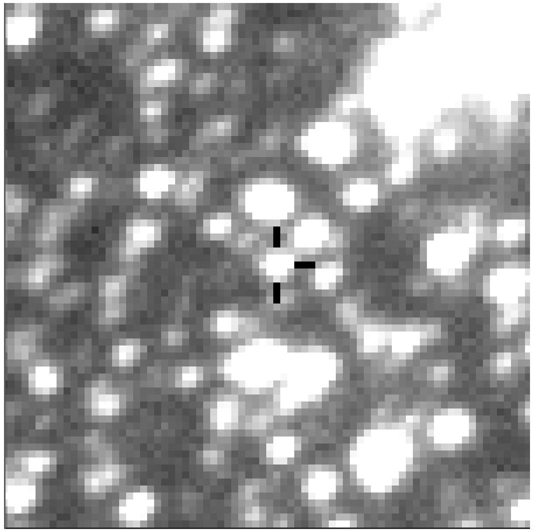

OGLE team discovered 14 planetary systems using this technique

Strong lensing history

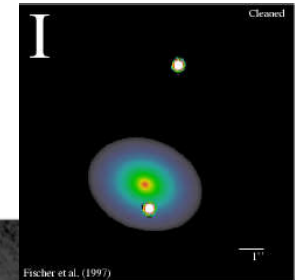

- **Revival** - Refsdal 1964 idea: H_0 can be measured from time delays
- Walsh, Carswell & Weynmann 1979 - QSO-0957+561A,B
- „mysterious” giant arcs around clusters A370,Cl2244 (Paczyński suggests gravitational lensing) Soucail, Fort, Mellier 1987 confirm it spectroscopically

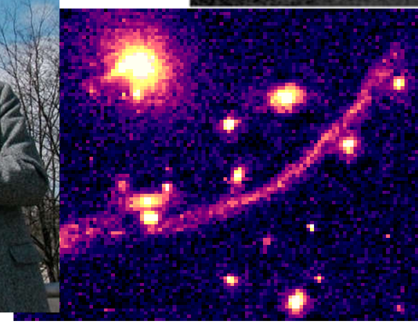

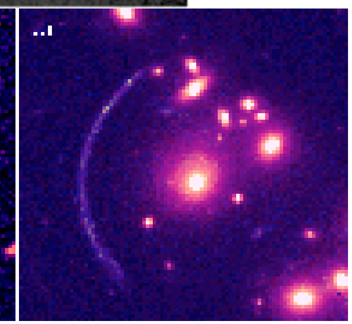

- in the period 1978 – 1992 only 11 lenses discovered
- 2006 about 70

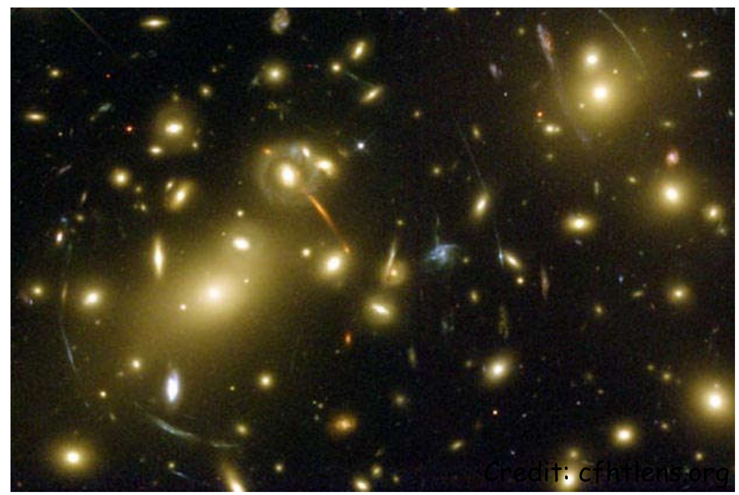

- now we have 300 strong lensing systems: ongoing surveys SLACS, BELLS, CFHT – SL2S, CLASS, SQLS, HAGGLeS, AEGIS, COSMOS, CASSOWARY

- in the future Pan-STARRS, LSST, JDES, SKA

Gravitational lensing

Light rays formalism

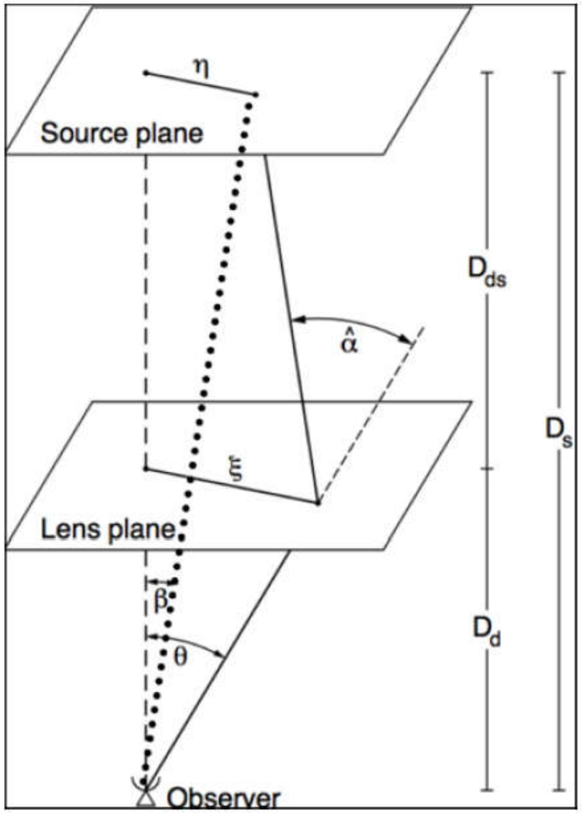

$$\hat{\boldsymbol{\alpha}}\left(\boldsymbol{\theta}\right) D_{ls} + \boldsymbol{\beta} D_s = \boldsymbol{\theta} D_s$$

$$\boldsymbol{\beta} = \boldsymbol{\theta} - \boldsymbol{\alpha}\left(\boldsymbol{\theta}\right)$$

gradient ψ_{2D}

Wavefronts formalism
(Fermat principle)

Light travels along a path extremalizing

time of flight $\int \frac{n}{c} \mathrm{d}l$

Lensing equation:

$$\vec{\theta} - \vec{\beta} - \frac{\partial \psi_{2D}}{\partial \vec{\theta}} = 0$$

Gravitational lensing

Wavefronts formalism
(Fermat principle)

index of refraction

$$\delta \int_A^B n(\vec{x}(l))\mathrm{d}l = 0$$

Light travels along a path extremalizing

time of flight $\int \frac{n}{c}\mathrm{d}l$

weak field limit of GR

$$\mathrm{d}s^2 = g_{\mu\nu}\mathrm{d}x^\mu \mathrm{d}x^\nu = \left(1 + \frac{2\Phi}{c^2}\right)c^2\mathrm{d}t^2 - \left(1 - \frac{2\Phi}{c^2}\right)(\mathrm{d}\vec{x})^2$$

null geodesics

$$\left(1 + \frac{2\Phi}{c^2}\right)c^2\mathrm{d}t^2 = \left(1 - \frac{2\Phi}{c^2}\right)(\mathrm{d}\vec{x})^2$$

$$c' = \frac{|\mathrm{d}\vec{x}|}{\mathrm{d}t} = c\sqrt{\frac{1+\frac{2\Phi}{c^2}}{1-\frac{2\Phi}{c^2}}} \approx c\left(1 + \frac{2\Phi}{c^2}\right)$$

$$n = c/c' = \frac{1}{1+\frac{2\Phi}{c^2}} \approx 1 - \frac{2\Phi}{c^2}$$

index of refraction

2-dimensional Newtonian potential – projected to the lens plane

$$\hat{\Psi}(\vec{\theta}) = \frac{D_{\mathrm{LS}}}{D_{\mathrm{L}}D_{\mathrm{S}}}\frac{2}{c^2}\int \Phi(D_{\mathrm{L}}\vec{\theta}, z)\mathrm{d}z$$

$$\vec{\theta} - \vec{\beta} - \frac{\partial \psi_{2D}}{\partial \vec{\theta}} = 0$$

Some Theory

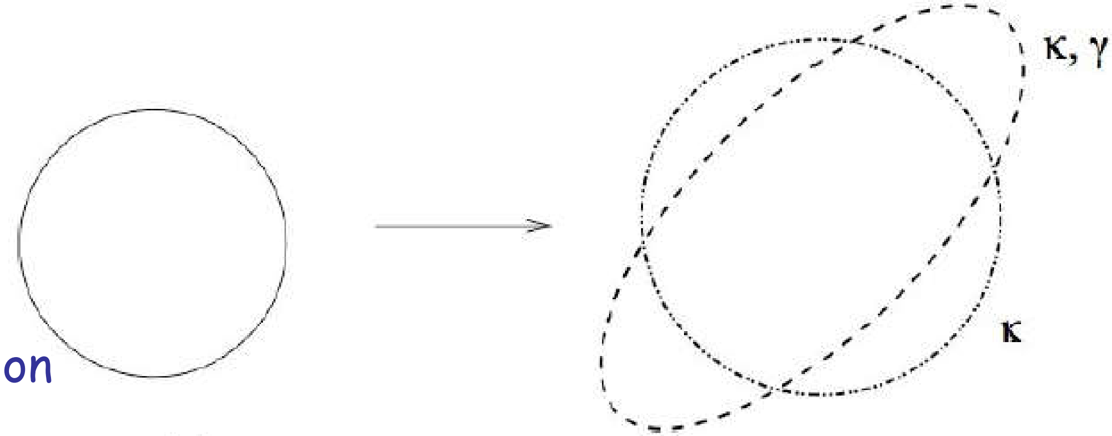

Jacobi matrix for the lens equation

$$\mathcal{A}(\vec{\theta}) = \frac{\partial \vec{\beta}}{\partial \vec{\theta}} = \left(\delta_{ij} - \frac{\partial^2 \psi(\vec{\theta})}{\partial \theta_i \partial \theta_j} \right)$$

convergence - isotropic

$$\nabla^2 \psi = 2\kappa$$

$$\mathcal{A}(\vec{\theta}) = \begin{pmatrix} 1-\kappa-\gamma_1 & -\gamma_2 \\ -\gamma_2 & 1-\kappa+\gamma_1 \end{pmatrix}$$

$$\gamma_1 = \frac{1}{2}\left(\frac{\partial^2 \psi}{\partial \theta_i^2} - \frac{\partial^2 \psi}{\partial \theta_j^2} \right)$$

shear - anisotropic

$$\gamma_2 = \frac{\partial^2 \psi}{\partial \theta_i \partial \theta_j}$$

$$\gamma \equiv \gamma_1 + \mathrm{i}\gamma_2 = |\gamma| \mathrm{e}^{2\mathrm{i}\varphi}$$

$$\mathcal{A}(\vec{\theta}) = (1-\kappa) \begin{pmatrix} 1 & 0 \\ 0 & 1 \end{pmatrix} - \gamma \begin{pmatrix} \cos 2\phi & \sin 2\phi \\ \sin 2\phi & -\cos 2\phi \end{pmatrix}$$

$$\mu \equiv \det M = \frac{1}{\det A} = \frac{1}{(1-\kappa)^2 - \gamma^2}$$

magnification

Gravitational lensing

Light rays formalism

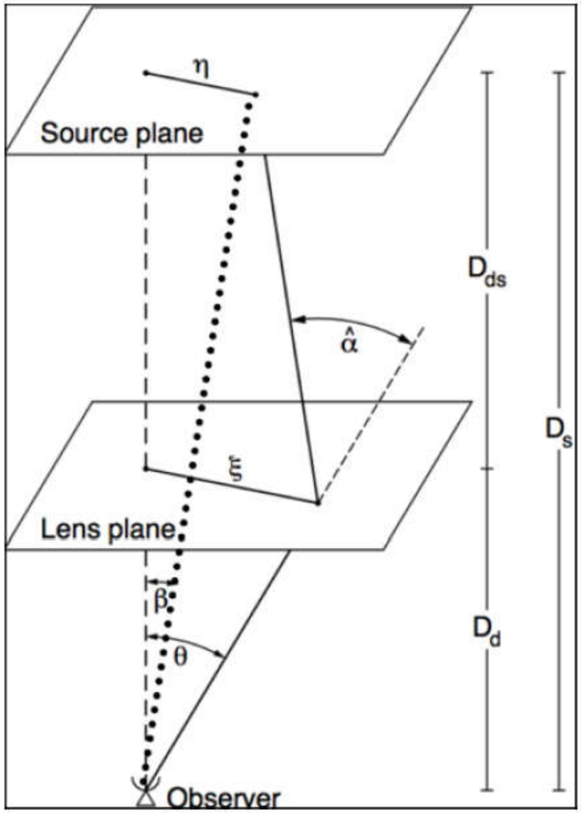

$$\hat{\boldsymbol{\alpha}}(\boldsymbol{\theta})\, D_{ls} + \boldsymbol{\beta} D_s = \boldsymbol{\theta} D_s$$

$$\boldsymbol{\beta} = \boldsymbol{\theta} - \boldsymbol{\alpha}(\boldsymbol{\theta})$$

gradient ψ_{2D}

Wavefronts formalism (Fermat principle)

caustics

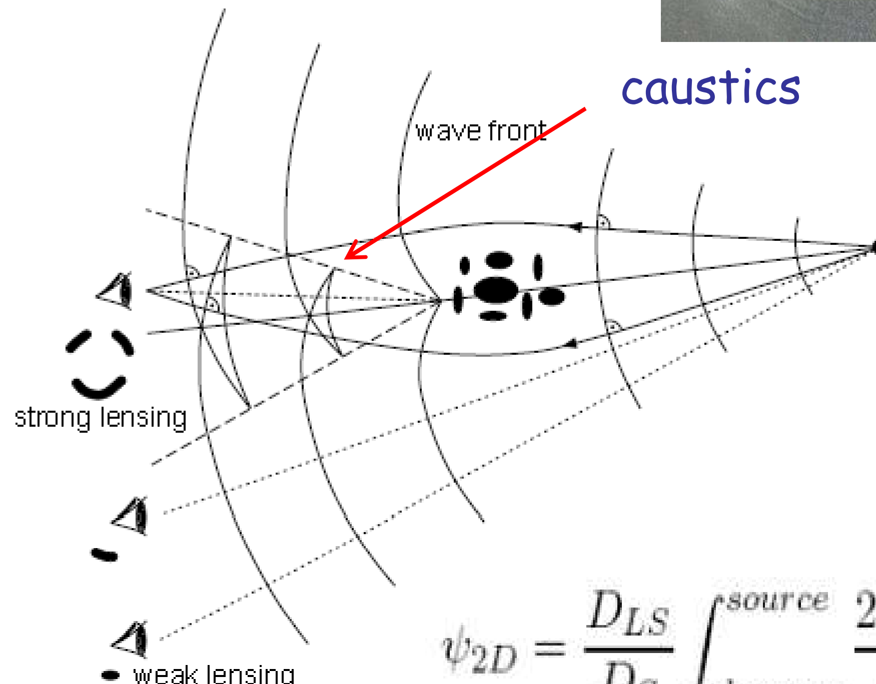

$$\psi_{2D} = \frac{D_{LS}}{D_S}\int_{observer}^{source}\frac{2\Phi_{3D}}{c^2}\frac{d\ell}{D_L}$$

$$\tau = \frac{1+z_L}{c}\frac{D_L D_S}{D_{LS}}\left[\frac{1}{2}(\vec{\theta}-\vec{\beta})^2 - \psi_{2D}(\vec{\theta})\right]$$

geometrical term

Shapiro effect

$$\nabla\tau(\boldsymbol{\theta};\boldsymbol{\beta}) = 0.$$

$$\vec{\theta} - \vec{\beta} - \frac{\partial\psi_{2D}}{\partial\vec{\theta}} = 0$$

Lens equation

Critical curves and caustics for the elliptic lens model

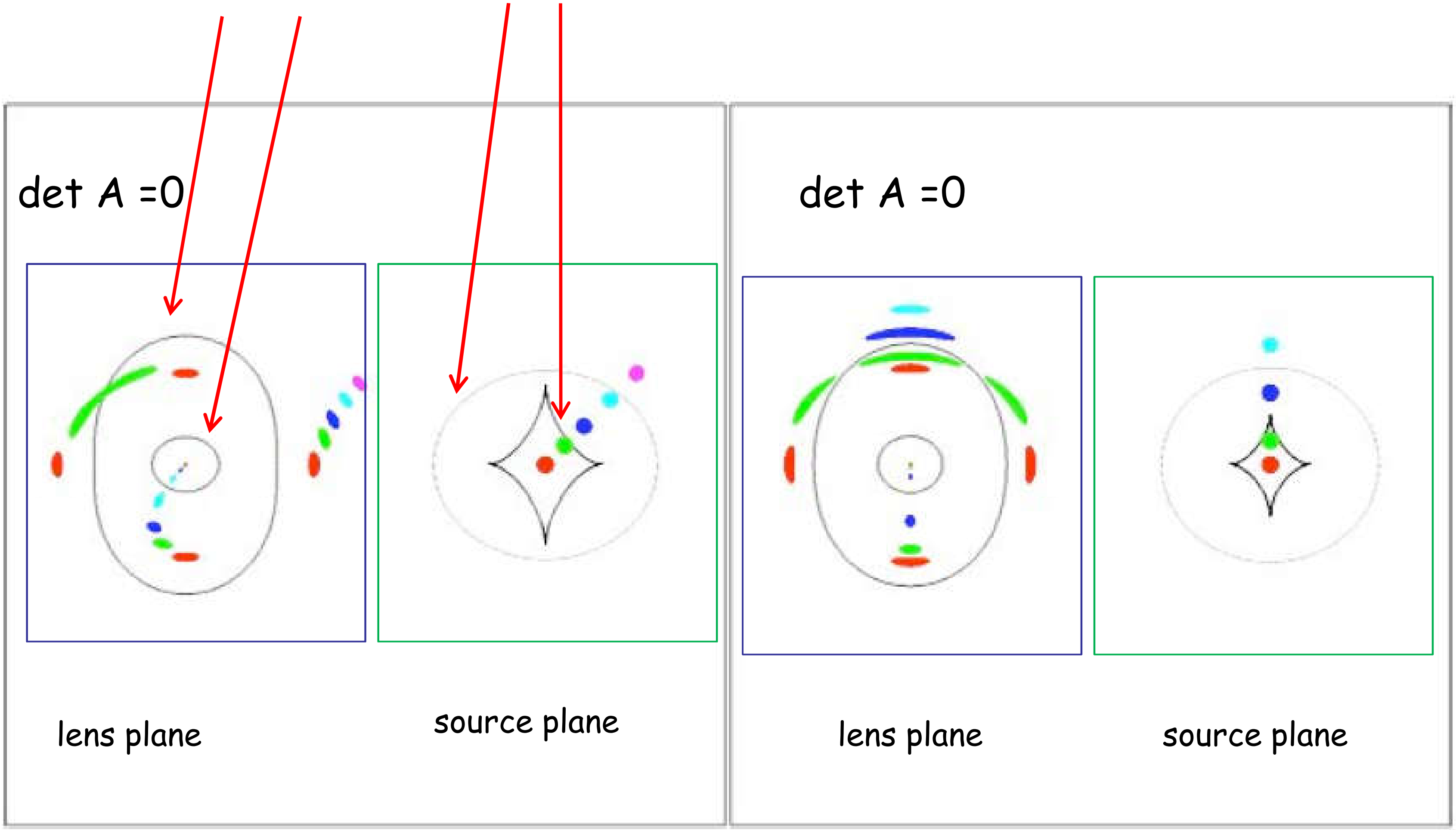

Recommended reading:

Quick yet comprehensive starters:

Massimo Meneghetti – Introduction to Gravitational Lensing (Lecture scripts)

http://www.ita.uni-heidelberg.de/~massimo/sub/Lectures/gl_all.pdf

Ramesh Narayan, Matthias Bartelmann – Lectures on Gravitational Lensing (1995 Jerusalem Winter School)

http://www.tau.ac.il/~lab3/MICROLENSING/JeruLect.pdf

Classical Books:

P. Schneider, J.Ehlers, E.E. Falco – Gravitational Lenses (Springer 1992)

Gravitational lensing: Strong, weak, and micro,
Saas-Fee Adv Courses
(ed.) Meylan, G., Jetzer, Ph., North P. (Berlin: Springer 2006)

Effect of gravitational lensing - summary

Two regimes of lensing:
Einstein radius
(determined by mass !)
- sets a characteristic
angular scale

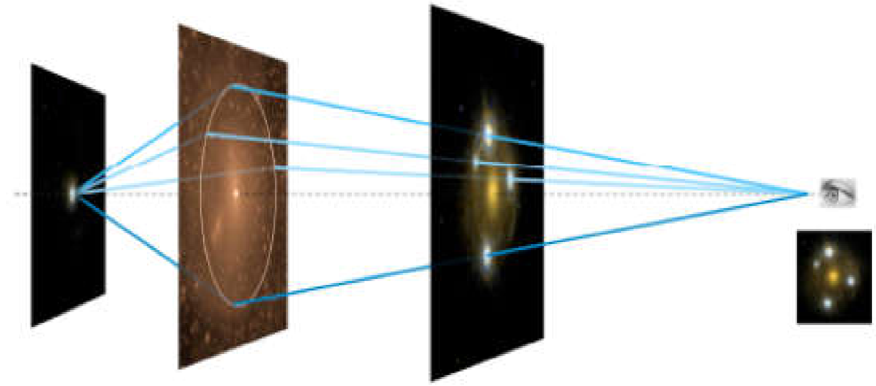

Strong:
• multiple images

• time delay between images
– method to determine H_0

• image amplification

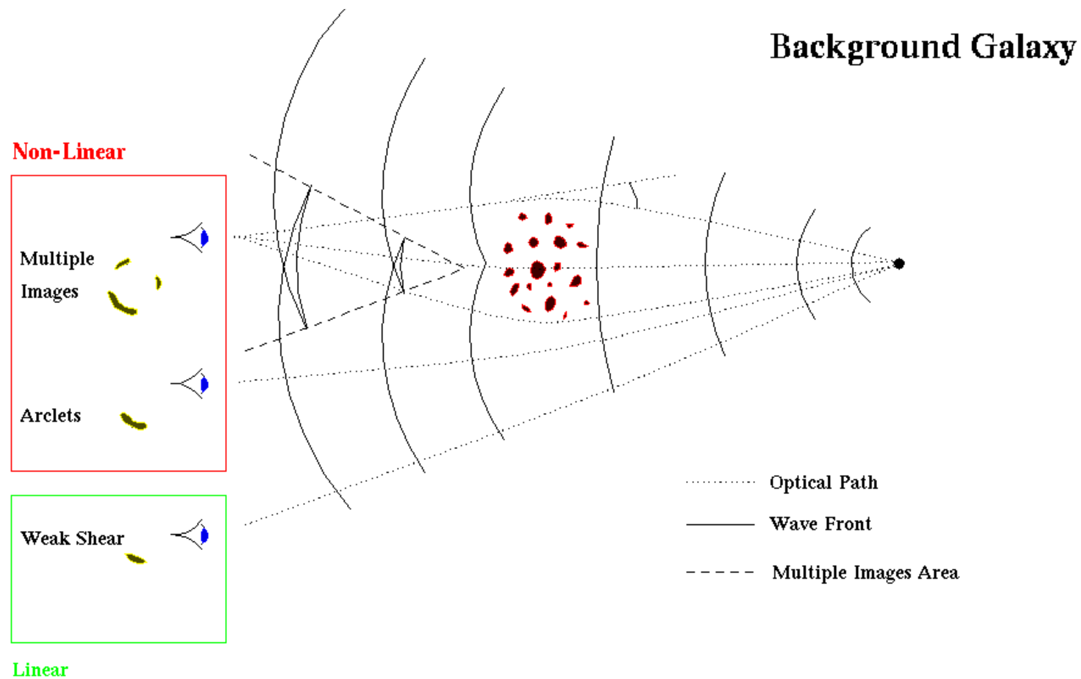

weak: distorsion of images

Application of strong lensing

Structure of galaxies in different evolutionary stages:

lenses as „cosmic telescopes"
lensing + stellar kinematics

Dark matter at galactic scale:

„missing" mass clumps at small scales
anomalous flux ratios
microlensing

Cosmology:

determining the Hubble constant
dark energy problem

Cosmic telescopes - gravitational lenses magnify the image of the source, unfortunately they strongly distort it

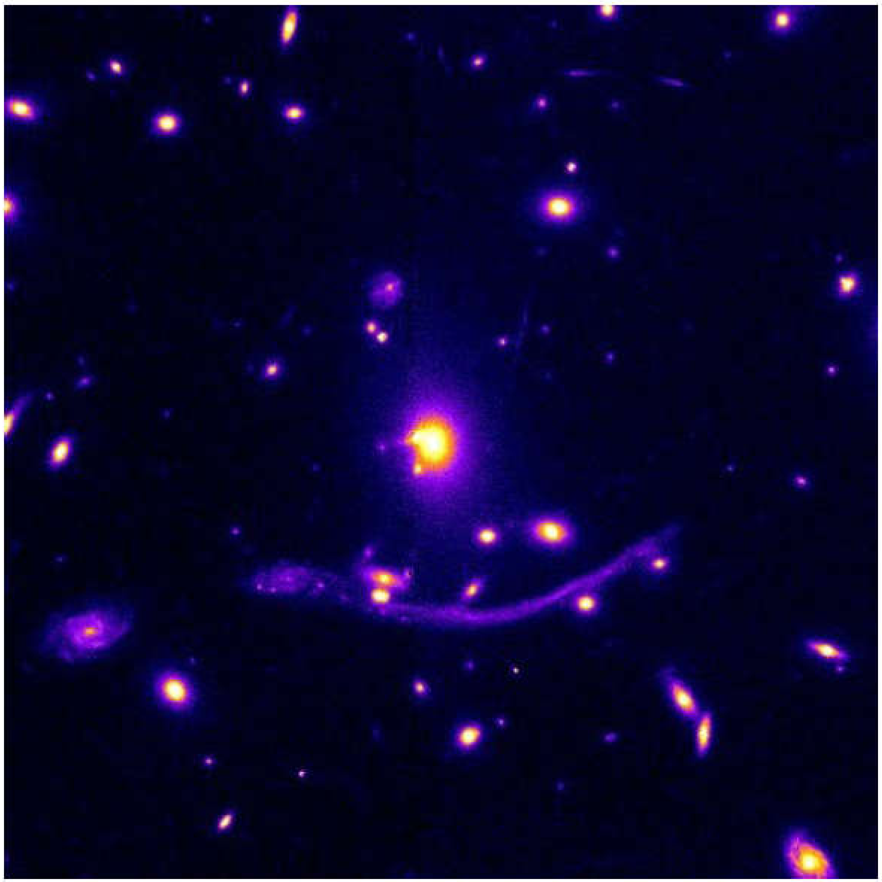

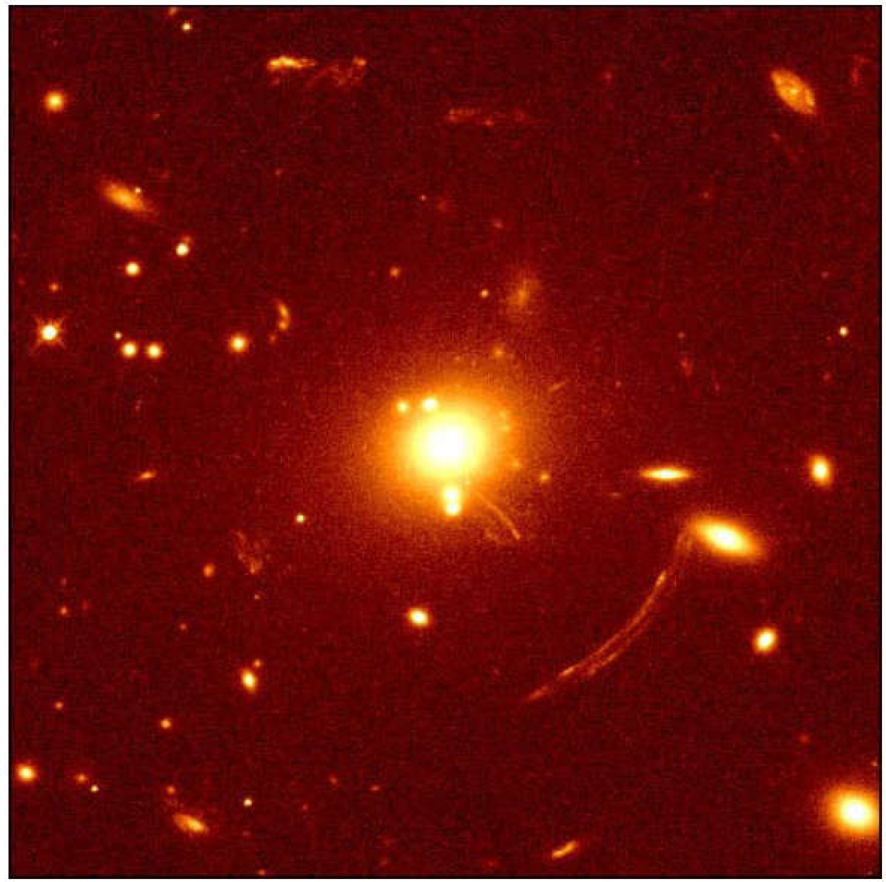

Cosmic telescopes

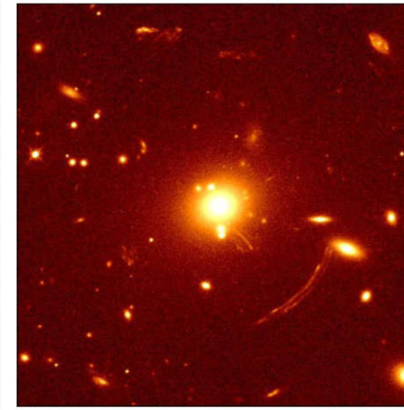

Gravitational lensing magnifies the distant universe

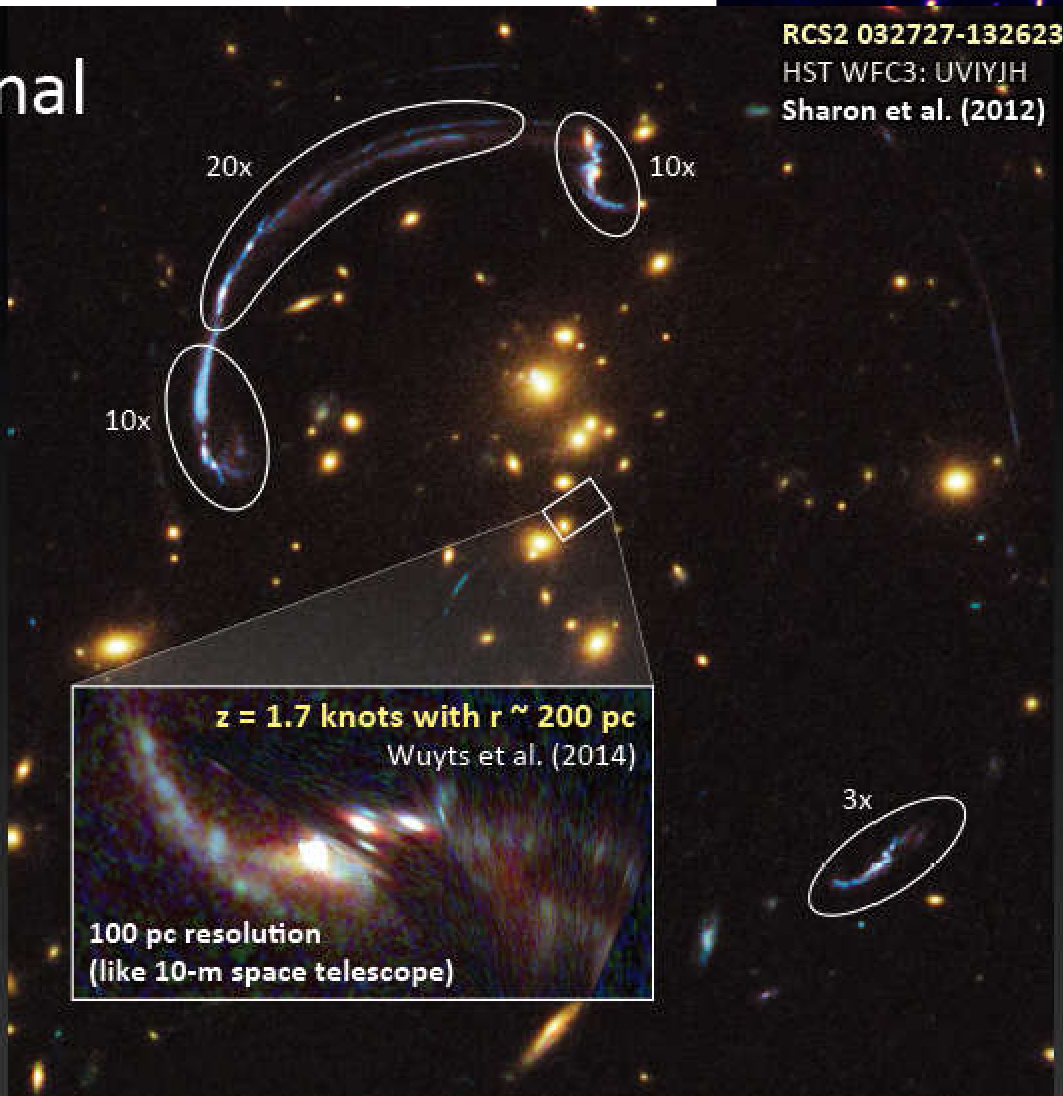

Coupling SL – internal kinematics

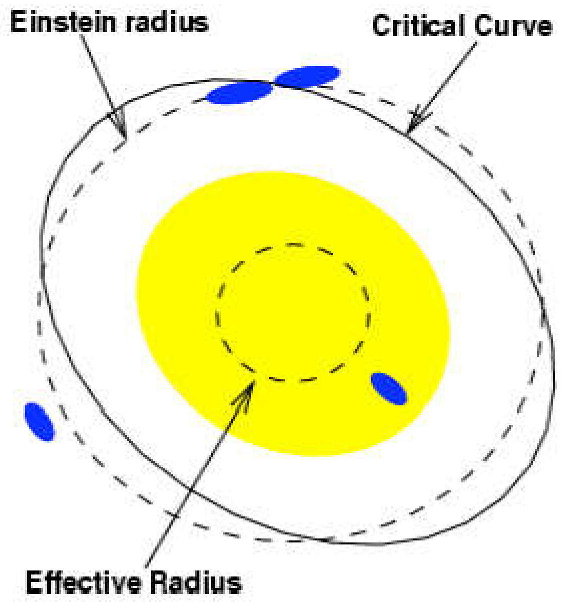

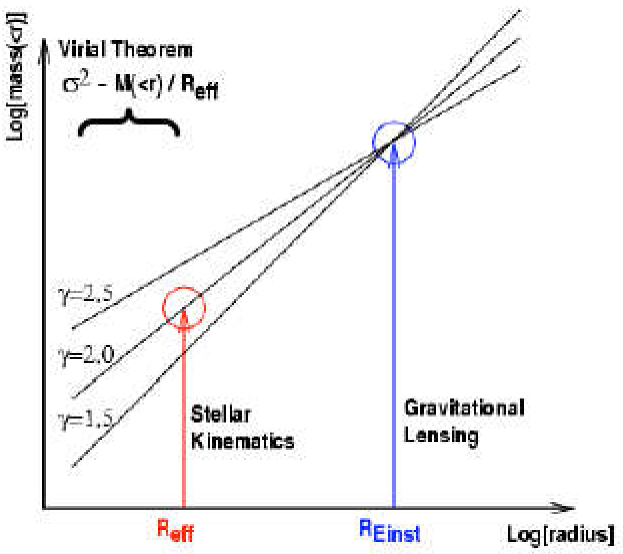

Einstein Radius = one point on mass profile

Internal kinematics within SDSS fiber aperture = another point on mass profile

Both methods only based on gravity (~few gas physics).

Some technical details - terminology

de Vaucouleurs profile

$$I(R) = I_e \exp[-7.67[(R/R_e)^{1/4} - 1]]$$

Effective radius R_e

radius of an isophote containing 1/2 of the total lumionosity

Central velocity dispersion

σ_{e2} (or σ_{e8}) = velocity dispersion inside $R_e/2$ (or $R_e/8$)

We have to correct for the aperture

$$\sigma_{e2} = \sigma_{ap} \left(\frac{R_{eff}}{2\,r_{ap}} \right)^{-0.04}$$

$$r_{ap} = (xy/\pi)^{1/2}$$

Slit is rectangular: x – width, y -length

Jeans Equation

spherical Jeans equation

$$\frac{1}{\nu}\frac{d\nu\sigma_r^2}{dr} + \frac{2\beta(r)}{r}\sigma_r^2 = -\frac{GM(r)}{r^2} \tag{B.90}$$

relates the radial velocity dispersion $\sigma_r = \langle v_r^2 \rangle^{1/2}$, the isotropy parameter $\beta(r) = 1 - \sigma_\theta^2/\sigma_r^2$ characterizing the ratio of the tangential dispersion to the radial dispersion, the luminosity density of the stars $\nu(r)$ and the mass distribution $M(r)$. A well known result from dynamics is that you cannot infer the mass distribution $M(r)$ without constraining the isotropy $\beta(r)$ (e.g. Binney & Mamon 1982). Models with $\beta = 0$ are called isotropic models (i.e. $\sigma_r = \sigma_\theta$), while models with $\beta \to 1$ are dominated by radial orbits ($\sigma_\theta \to 0$) and models with $\beta \to -\infty$ are dominated by tangential orbits ($\sigma_r \to 0$) .

GRAVITATIONAL LENSING & STELLAR DYNAMICS

Mass Profiles and Shapes of Cosmological Structures
G. Mamon, F. Combes, C. Deffayet, B. Fort (eds)
EAS Publications Series, Vol. ?, 2005

Koopmans, L.V.E.[1]

2.1 Combining Lensing Mass and Stellar Velocity Dispersions

Let us suppose the following spherical scale-free model for the lens galaxy:

$$\begin{cases} \nu_l(r) & = & \nu_{l,0} r^{-\delta} \\ \nu_\rho(r) & = & \nu_{\rho,0} r^{-\gamma'} \\ \beta(r) & = & 1 - \langle\sigma_\theta^2\rangle / \langle\sigma_r^2\rangle \end{cases} , \tag{2.1}$$

where $\nu_l(r)$ is the luminosity density of stars – a trace component – embedded in a total (i.e. luminous plus dark-matter) mass distribution with a density $\nu_\rho(r)$. The anisotropy of the stellar velocity ellipsoid is β, constant with radius. For a lens galaxy with a projected mass $M_{\rm E}$ inside the Einstein radius $R_{\rm E}$, the luminosity weighted average line-of-sight velocity dispersion inside an aperture $R_{\rm A}$ is given, after solving the spherical Jeans equations, by

$$\langle\sigma_{||}^2\rangle(\leq R_{\rm A}) = \frac{1}{\pi}\left[\frac{GM_{\rm E}}{R_{\rm E}}\right] f(\gamma', \delta, \beta) \times \left(\frac{R_{\rm A}}{R_{\rm E}}\right)^{2-\gamma'} , \tag{2.2}$$

where

$$f(\gamma', \delta, \beta) = 2\sqrt{\pi}\left(\frac{\delta - 3}{(\xi - 3)(\xi - 2\beta)}\right) \times \left\{\frac{\Gamma[(\xi-1)/2]}{\Gamma[\xi/2]} - \beta\frac{\Gamma[(\xi+1)/2]}{\Gamma[(\xi+2)/2]}\right\} \times \left\{\frac{\Gamma[\delta/2]\Gamma[\gamma'/2]}{\Gamma[(\delta-1)/2]\Gamma[(\gamma'-1)/2)]}\right\} \tag{2.3}$$

with $\xi = \gamma' + \delta - 2$. Similarly,

$$\sigma_{||}^2(R) = \frac{1}{\pi}\left[\frac{GM_E}{R_E}\right]\left(\frac{\xi - 3}{\delta - 3}\right) f(\gamma', \delta, \beta) \times \left(\frac{R}{R_E}\right)^{2-\gamma'} . \quad (2.4)$$

In the simple case of a SIS with $\gamma' = \delta = \xi = 2$ and $\beta = 0$, we recover the well-known result

$$\sigma_{||}^2(R) = \frac{1}{\pi}\left[\frac{GM_E}{R_E}\right] \quad \text{(SIS)}, \quad (2.5)$$

Now, the idea is that

mass inside Enstein radius calculated from lensing

$$M_l = \frac{c^2}{4G}\frac{D_l D_s}{D_{ls}}\theta_E{}^2$$

should be equal to mass inside Einstein radius calculated from dynamics

$$M_d = \frac{\pi}{G}\sigma_0{}^2 R_E\left(\frac{R_E}{R_{ap}}\right)^{2-\gamma} f(\gamma, \delta, \beta)$$

The density slope of E/S0 galaxies between z=0.08-0.33

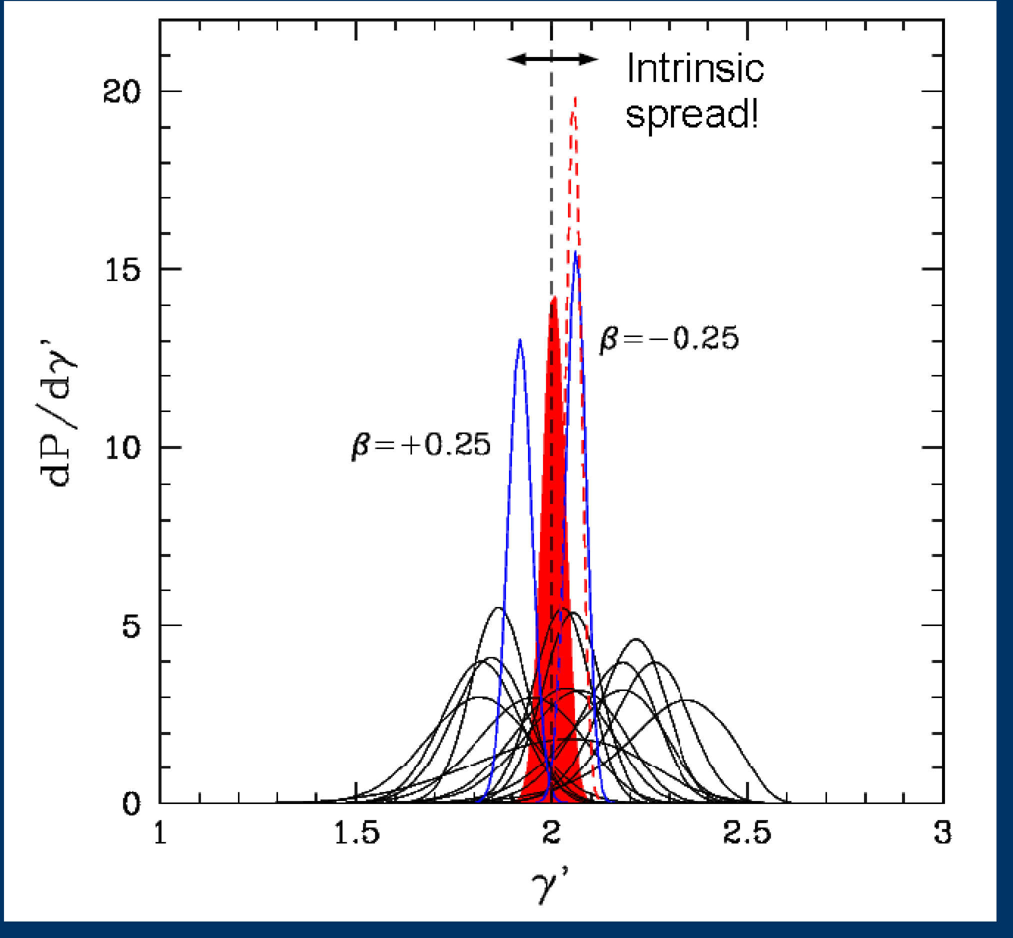

(Koopmans et al. 2006)

Total density slope inside ~0.3-1.0 R_{eff}

$\langle\gamma'\rangle = 2.01 \pm 0.03$

ML analysis:
Intrinsic spread is only 6%
(similar to Gerhard et al. 2001)

After L. Koopmans : *www.angles.eu.org/meetings/mid_term/copenhagen_leon.pdf*

THE SL2S GALAXY-SCALE LENS SAMPLE. II. COSMIC EVOLUTION OF DARK AND LUMINOUS MASS IN EARLY-TYPE GALAXIES

ANDREA J. RUFF[1,2*], RAPHAËL GAVAZZI[3], PHILIP J. MARSHALL[1,4], TOMMASO TREU[1†], MATTHEW W. AUGER[1], AND FLORENCE BRAULT[3]

(2011) ApJ, 727, 96

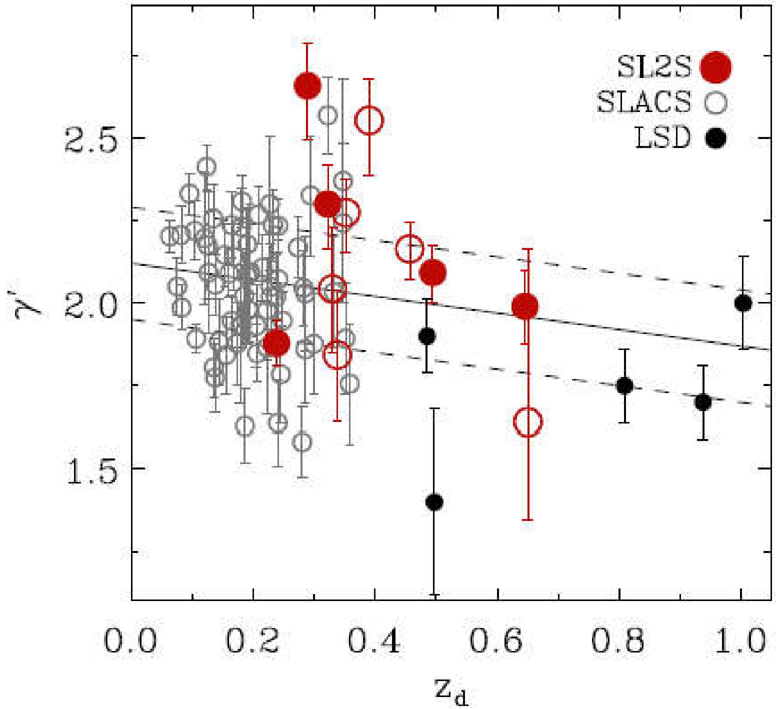

FIG. 13.— Cosmic evolution of total mass density slope, γ'. The SLACS and LSD values were taken from: (Auger et al. 2010) and (Treu & Koopmans 2002; Koopmans & Treu 2003; Treu & Koopmans 2004), respectively. The error bars show the 16th and 84th percentiles. The best fit to the data is shown by the solid line and the scatter is shown by the dashed lines.

We quantify this statement by fitting the $\gamma'(z_d)$ data with a linear relation in the mean slope, still including Gaussian scatter about that relation:

$$\langle\gamma'\rangle(z_d) = \langle\gamma'_0\rangle + \frac{\partial\langle\gamma'\rangle}{\partial z_d} z_d \pm S_{\gamma'}. \qquad (15)$$

For the SL2S data alone, we find $\langle\gamma'_0\rangle = 2.22^{+0.17}_{-0.21}$, $\partial\langle\gamma'\rangle/\partial z_d = -0.16^{+0.48}_{-0.51}$ for the gradient and, in this

evolving γ' case, the scatter is $S_{\gamma'} = 0.23^{+0.09}_{-0.06}$. When we include the SLACS and LSD data points, we find $\langle\gamma'_0\rangle = 2.12^{+0.03}_{-0.04}$, $\partial\langle\gamma'\rangle/\partial z_d = -0.25^{+0.10}_{-0.12}$, and $S_{\gamma'} = 0.17^{+0.02}_{-0.02}$.

THE BOSS EMISSION-LINE LENS SURVEY. II. INVESTIGATING MASS-DENSITY PROFILE EVOLUTION IN THE SLACS+BELLS STRONG GRAVITATIONAL LENS SAMPLE[1]

Adam S. Bolton[2], Joel R. Brownstein[2], Christopher S. Kochanek[3], Yiping Shu[2], David J. Schlegel[4], Daniel J. Eisenstein[5], David A. Wake[6], Natalia Connolly[7], Claudia Maraston[8], Ryan A. Arneson[2,9], and Benjamin A. Weaver[10]

(2012) ApJ, 744, 41

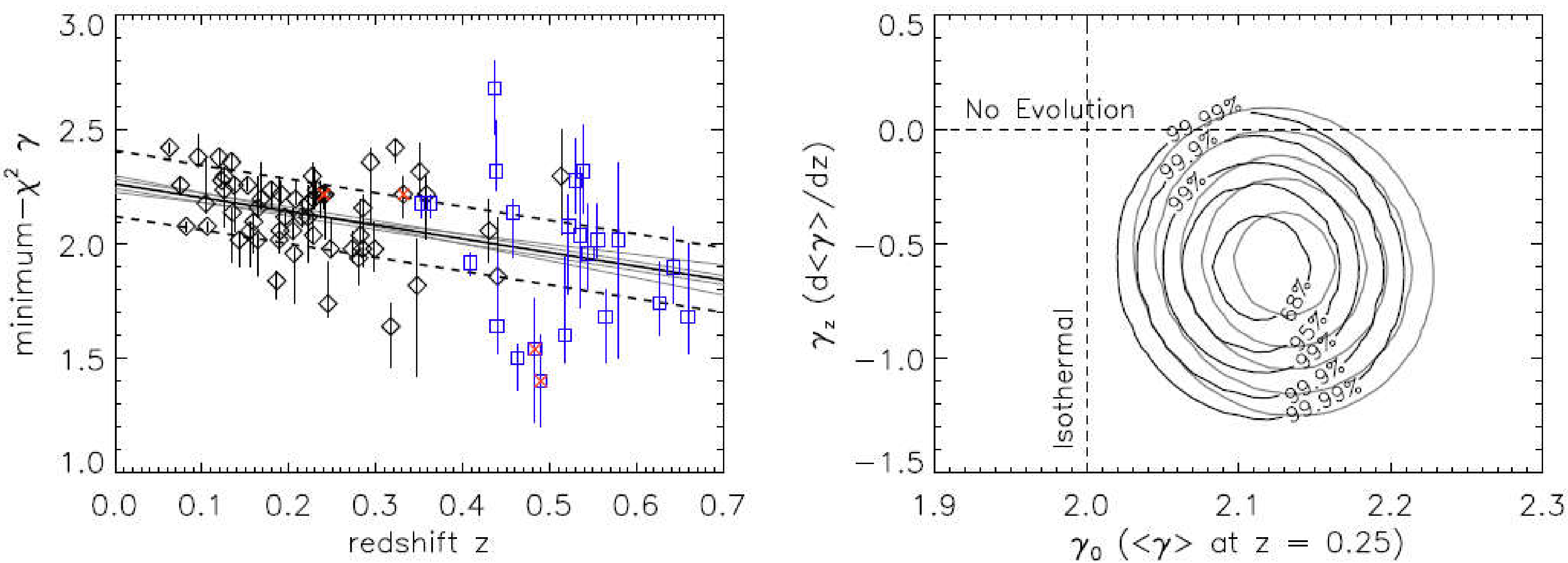

Fig. 2.— *Left:* Minimum-χ^2 values for the logarithmic total mass-density profile slope γ for SLACS (black diamonds) and BELLS (blue squares) lenses. Error bars indicate $\Delta\chi^2 = 1$. The solid line shows the best-fit relation, gray lines indicate the "1-sigma" error in the slope and zero-point of this relation, and dashed lines indicate the best-fit intrinsic RMS population scatter. Red crosses indicate systems with a maximum-likelihood log-velocity dispersion ($\log_{10} \sigma_e$, in km s^{-1}) either greater than 2.5 or less than 2.2 (see Figure 3.) Data points and error bars are for illustrative purposes only: the population parameter fits are done using the full $\chi^2(\gamma)$ function for each lens, as described in §3. *Right:* Posterior probability contours enclosing credible regions for the zero-point and evolution of the logarithmic mass-density slope parameter γ. Black curves are for the Nuker profile-based analysis; gray curves are for a de Vaucouleurs profile-based analysis.

The existence of dark matter in other galaxies

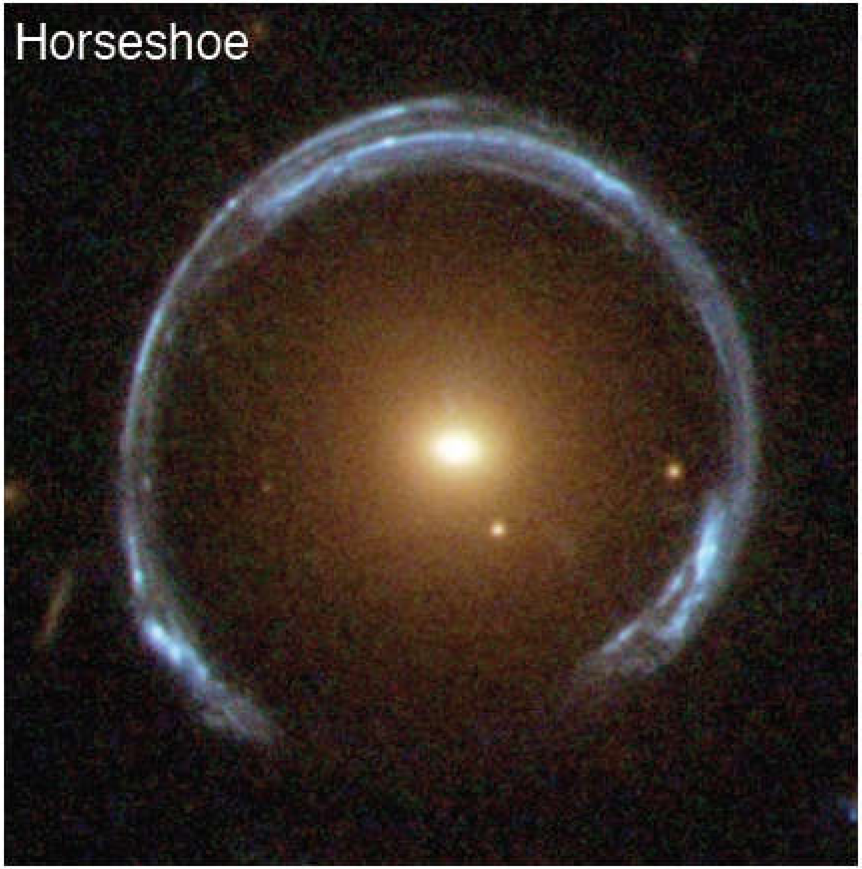

The Horseshoe system has a very large R_{einst}=30 kpc but only a single galaxy in the center suggesting an extremely massive DM halo.

Table 1. Properties of the cosmic Horseshoe[1].

	Parameter	Values
Lens Galaxy	RA	11h 48m 33.15s
	Dec	19° 30′ 03.″5
	Redshift	0.444
	Effective radii	1.″96 ± 0.″02
	g_L	(20.84 ± 0.06) mag
	r_L	(19.00 ± 0.02) mag
	i_L	(18.22 ± 0.01) mag
	z_L	(17.75 ± 0.04) mag
	Axis ratio, q	0.8 ± 0.1
Source	Redshift[2]	2.38115 ± 0.00012
	Star formation rate	$\sim 100\ M_\odot\ \mathrm{yr}^{-1}$
	Dynamical mass	$M_{vir} \simeq 10^{10}\ M_\odot$
Ring	Diameter	10.″2
	Length	~ 300°
	u_L	21.6 mag
	g_L	20.1 mag
	i_L	19.7 mag
	Mass enclosed[3]	$(5.02 \pm 0.09) \times 10^{12}\ M_\odot$

[1] Belokurov et al. (2007) measured the redshift of the source to be $z = 2.379$. We find a systematic shift that brings the source redshift to be $z = 2.3811$ in agreement with Quider et al. (2009).

[2] The mass within the Einstein radius or, more precisely, within the ring diameter, is taken from Dye et al. (2008).

[3] Parameters obtained from images taken with the 2.5 m Isaac Newton Telescope (INT). Magnitudes are taken from SDSS DR7. See Belokurov et al. (2007)

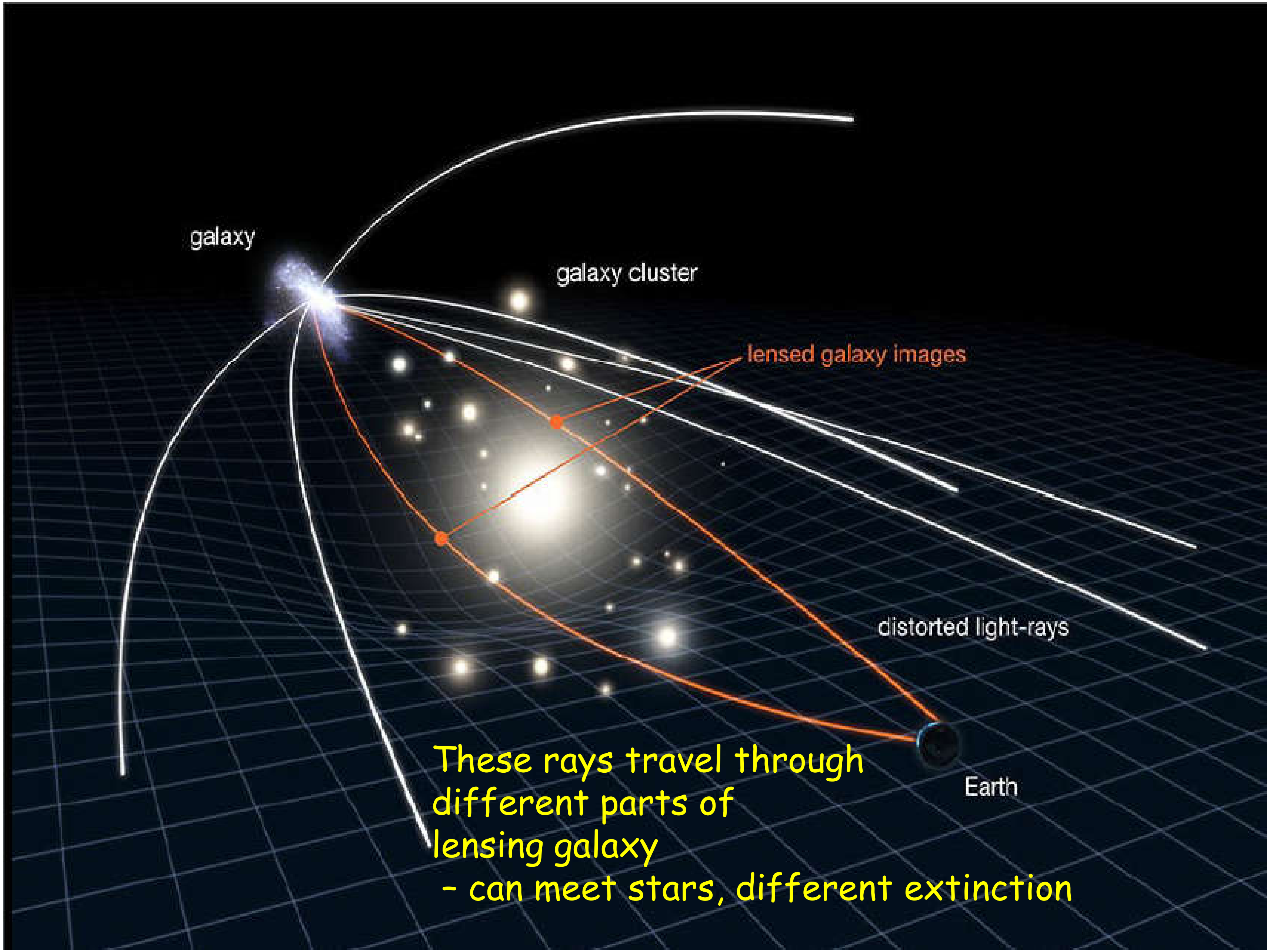
galaxy
galaxy cluster
lensed galaxy images
distorted light-rays
Earth
These rays travel through
different parts of
lensing galaxy
- can meet stars, different extinction

Cosmological application of strong lensing: dark matter mass distribution in galaxies

mass distribution

in galactic scales

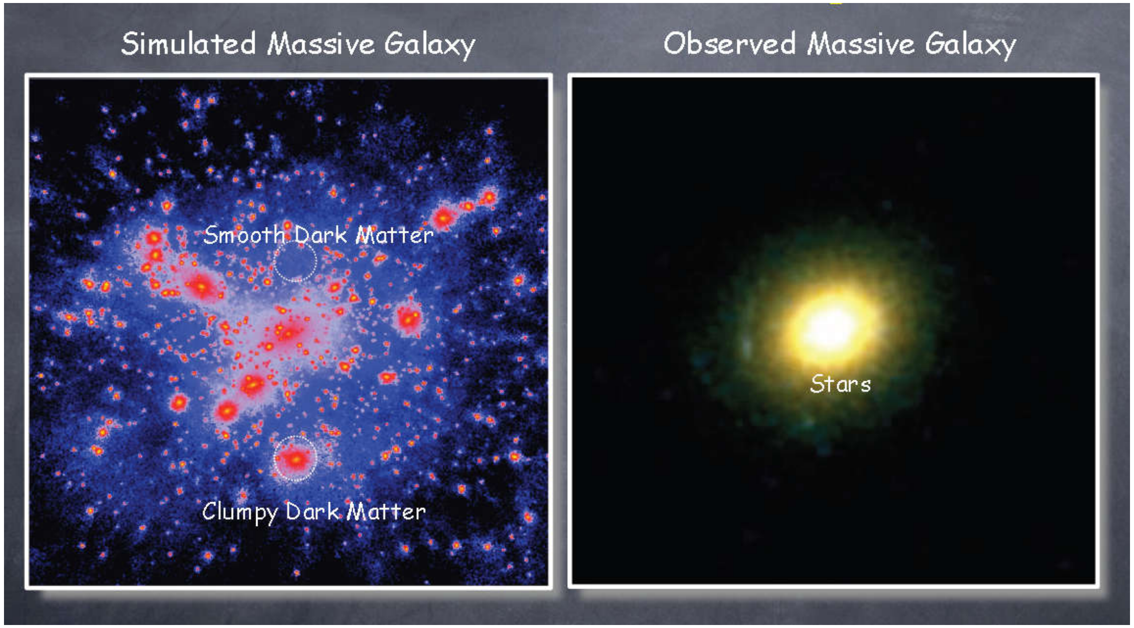

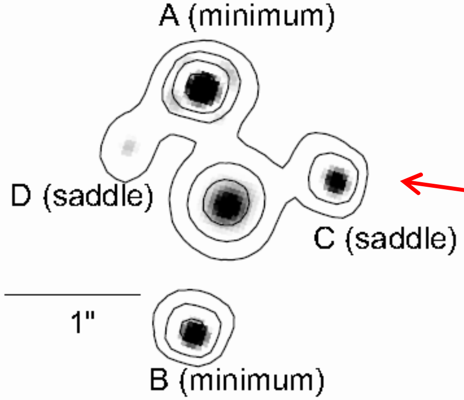

different brightness
of macro-images;

Theory predicts
their magnifications

Flux anomalies

Effect
due to lensing
by dark matter
clumps (?)

Time delays between images – proportional to H_0^{-1}

Variable source (AGN) + time delays → light curves of images

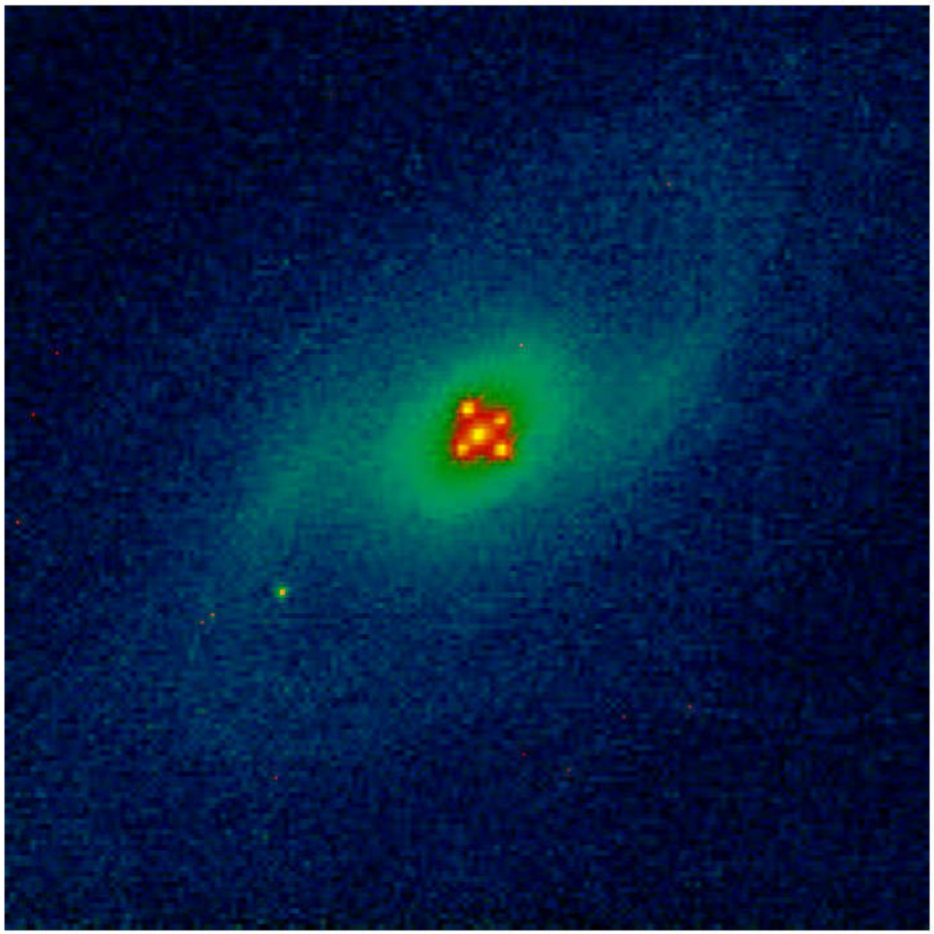

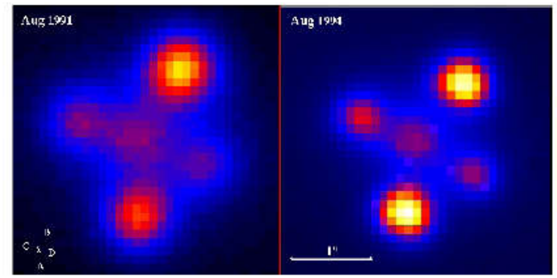

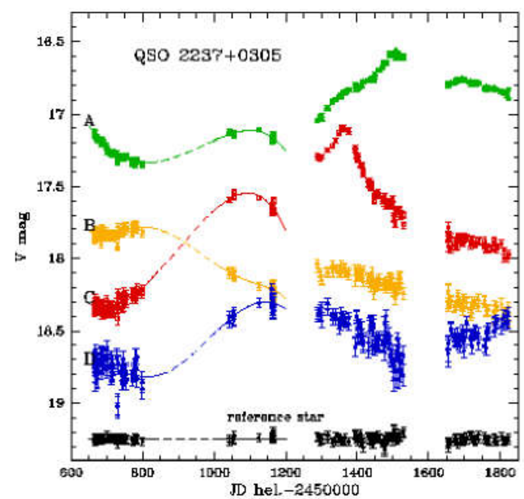

Simulated microlensing of a quasar

Lightcurves corresponding to 3 paths of the source over the caustics

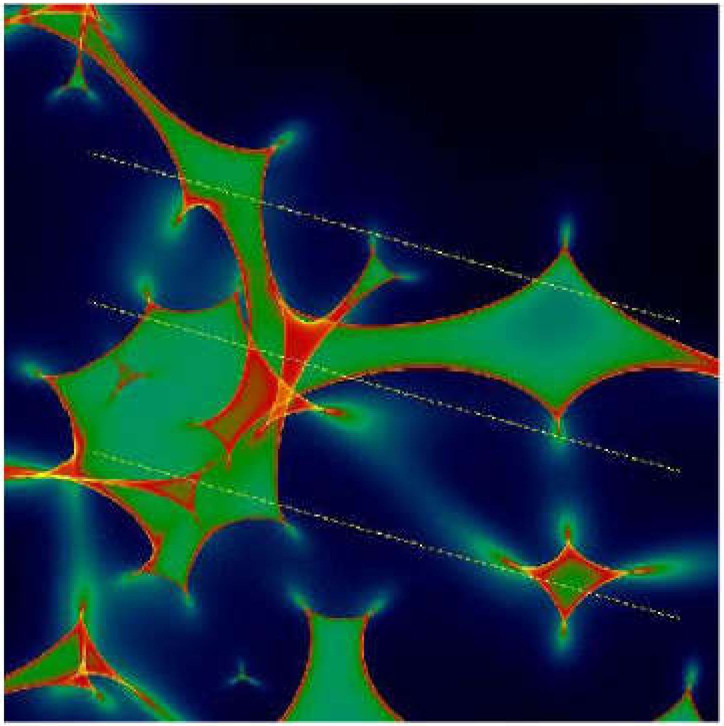

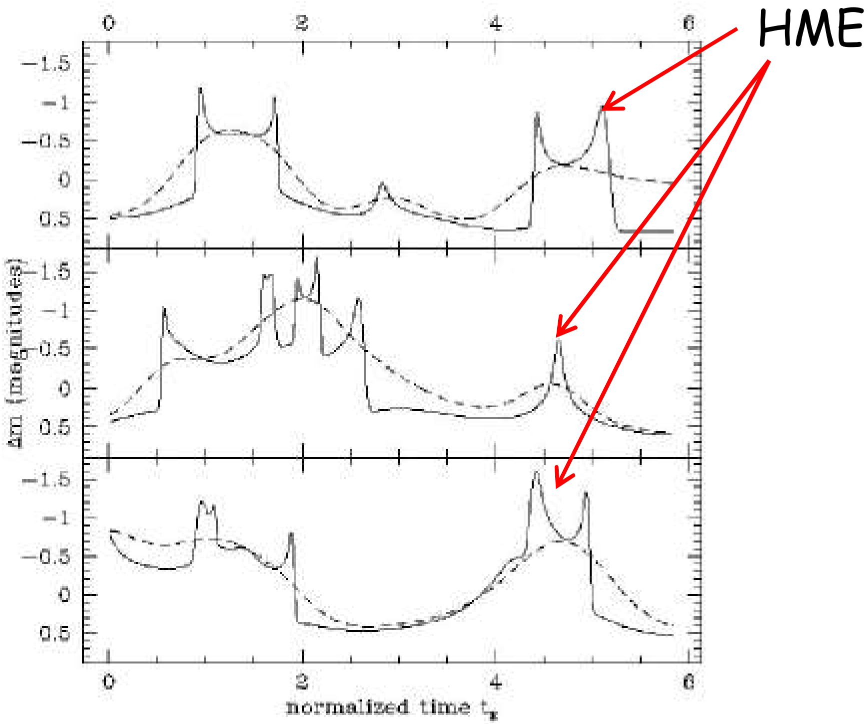

Caustic system generated by a simulated distribution of stars

Microlensing of macro-images

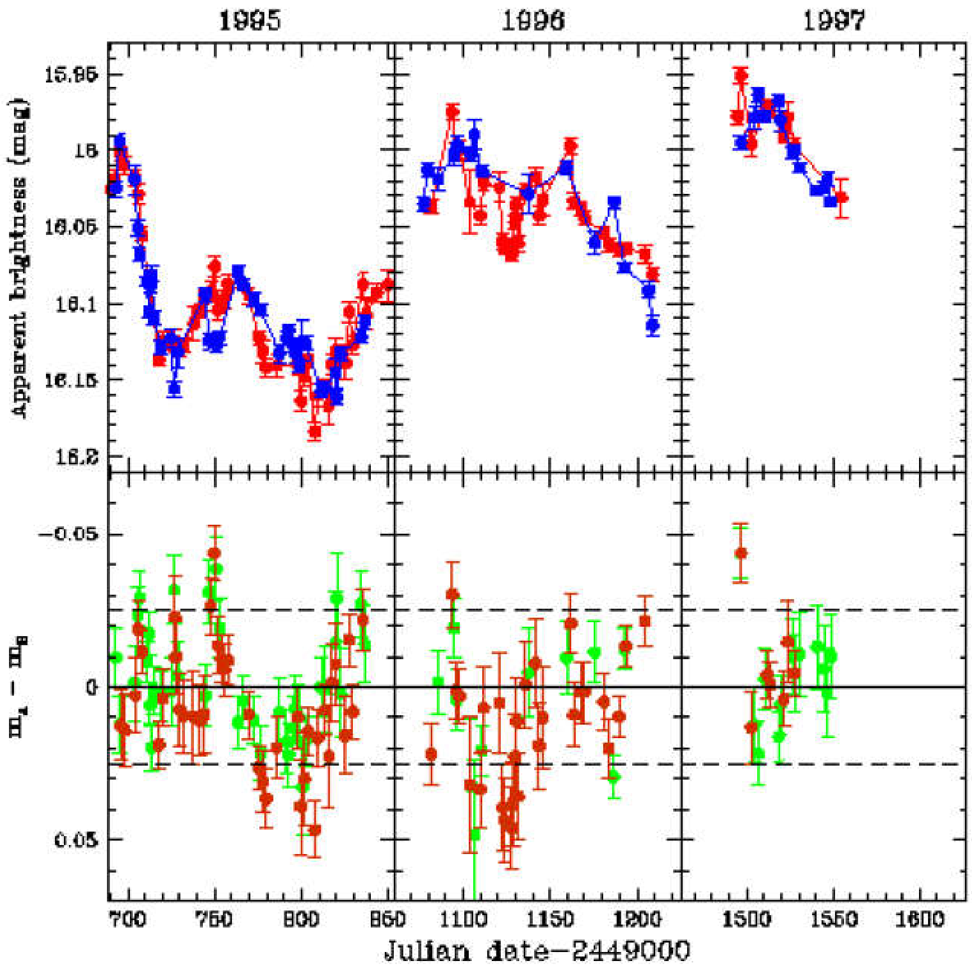

Lightcurves of macro-images superimposed after shifted by time delay (and corrected for image magnification)

Microlensing

residuals after subtracting lightcurves of macro-images

Fig. 47. Observed lightcurves of the double quasar Q0957+561; top: superposition of lightcurves of image A and (time shifted and magnitude shifted) image B; bottom: difference lightcurves (Wambsganss et al. 2000)

„Refsdal" supernova

„Refsdal supernova" discovered 11 Nov. 2014
Kelly et al. (2015) *Science* 347,1123

z=0.54 elliptical galaxy belonging to MACS J1149.6+2223 cluster

z = 1.49 source – spiral galaxy

host of SNII

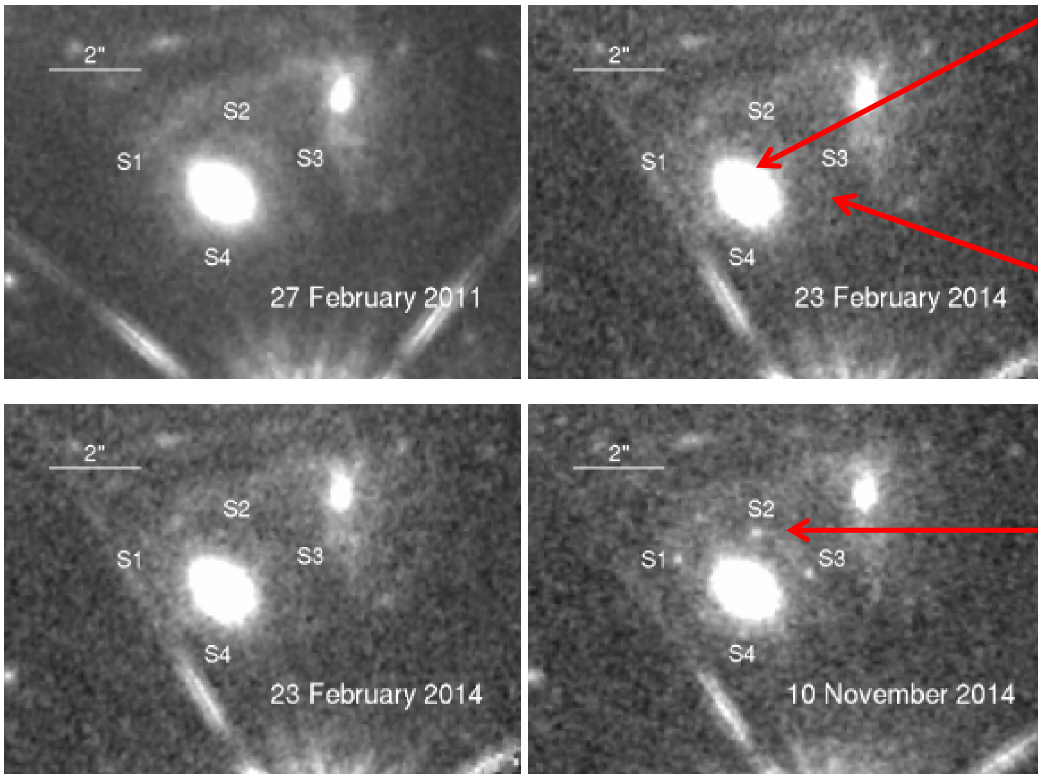

Fig. S4: Images of the lensing system from archival *HST* WFC3-IR observations in the *F140W* filter. All exposures obtained prior to 3 November 2014 show no evidence for variability at any of the positions associated with SN Refsdal.

„Refsdal" supernova

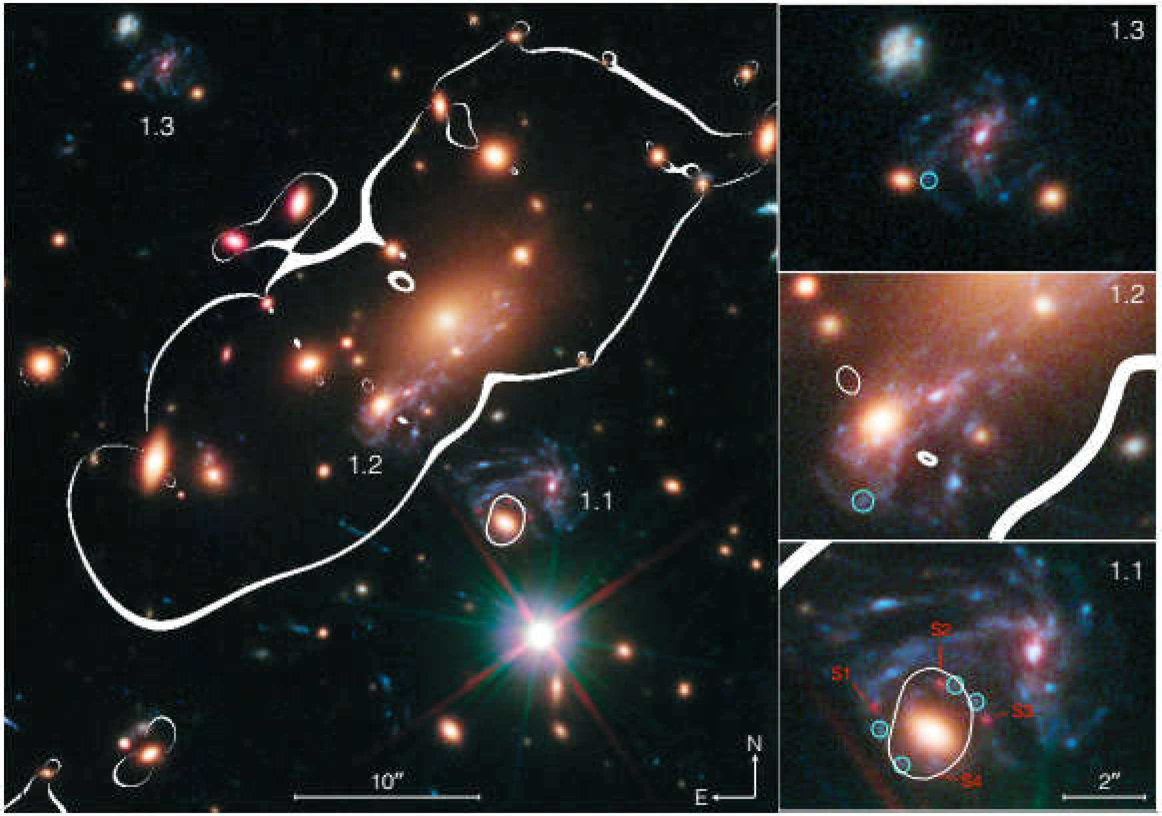

Fig. 2: Color-composite image of the galaxy cluster MACSJ1149.6+2223, with critical curves for sources at the $z = 1.49$ redshift of the host galaxy overlaid. Three images of the host galaxy formed by the cluster are marked with white labels (1.1, 1.2, and 1.3) in the left panel, and each is enlarged at right. The four current images of SN Refsdal that we detected (labeled S1 to S4 in red) appear as red point sources in image 1.1. Our model indicates that an image of the SN appeared in the past in image 1.3, and that one will appear in the near future in image 1.2. The extreme red hue of the SN may be somewhat exaggerated, because the blue and green channels include only data taken before the SN erupted. In image 1.1, both a single bright blue knot (cyan circles) and SN Refsdal are multiply imaged into four distinct locations. The image combines infrared and optical *HST* imaging data from the Frontier Fields and GLASS programs, along with images from the CLASH and the FrontierSN programs (GO-13790, PI: S.A.R.).

future reappearance expected in ca. 1 yr

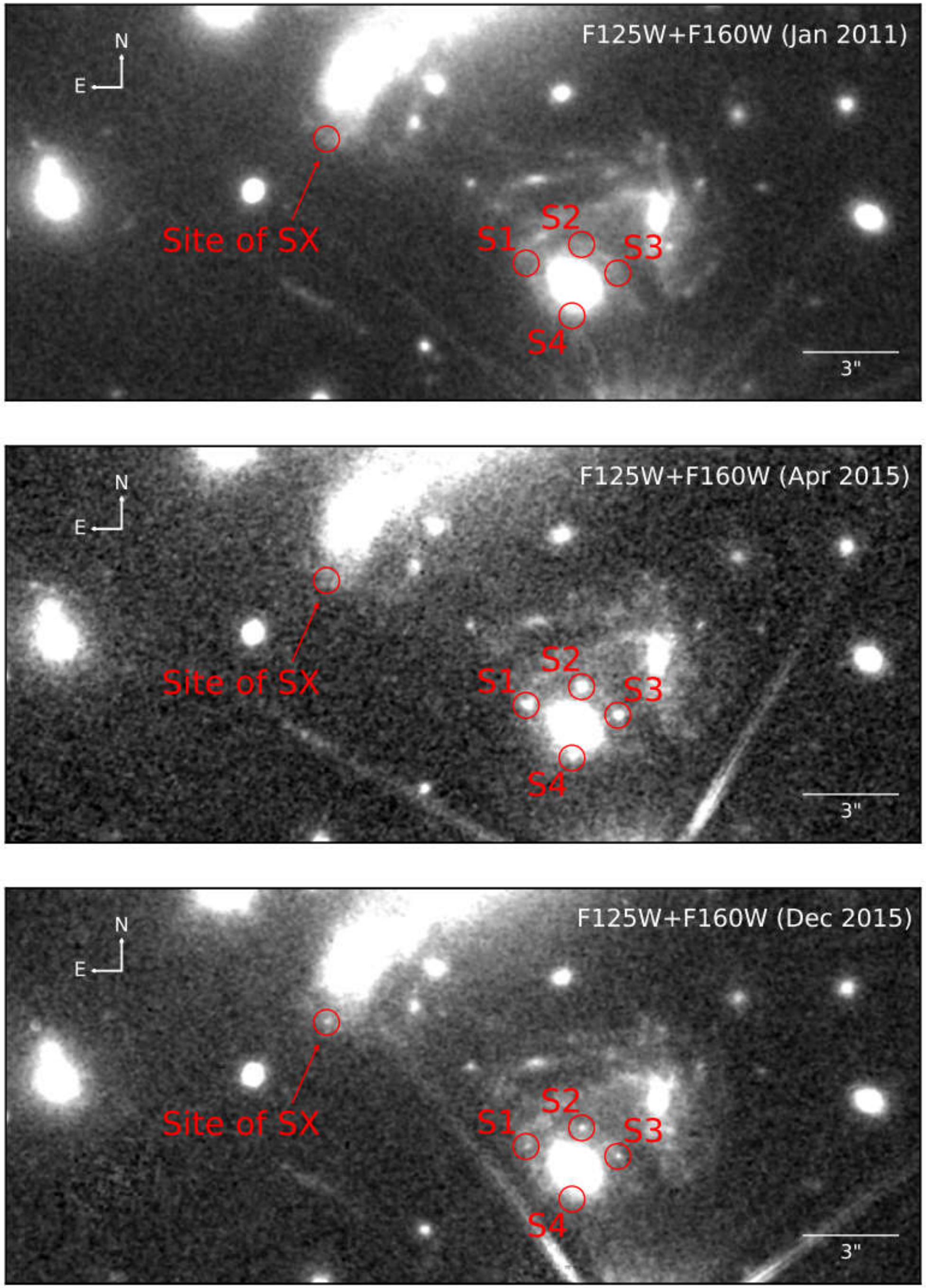

Kelly et al. (2016) *ApJL*

11 Dec. 2015
SNII found in SX image as predicted !!!

Great success of GR (mass distribution modeling from strong lensing)

Application of strong lensing

Structure of galaxies in different evolutionary stages:

- lenses as „cosmic telescopes"
- lensing + stellar kinematics

Dark matter at galactic scale:

- „missing" mass clumps at small scales
- anomalous flux ratios
- microlensing

Cosmology:

- determining the Hubble constant
- dark energy problem

Cosmology with strong lensing time delay

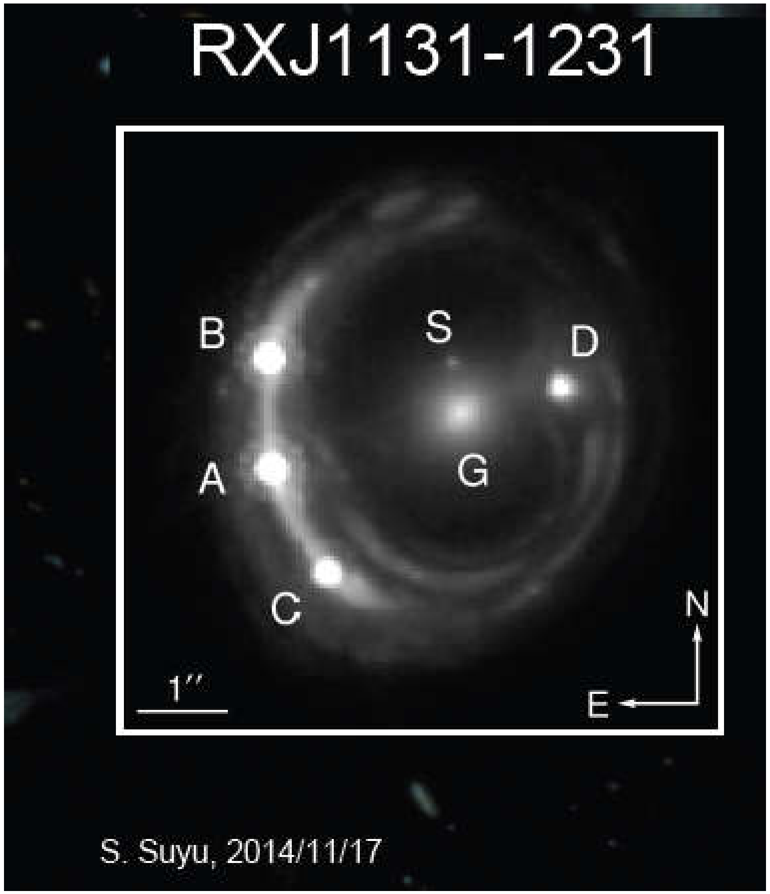

Time delay distance

Shapiro delay

$$t(\vec{\theta}) = \frac{(1+z_{\rm d})}{c}\frac{D_{\rm d}D_{\rm s}}{D_{\rm ds}}\left[\frac{1}{2}(\vec{\theta}-\vec{\beta})^2-\psi(\vec{\theta})\right]$$

Excess time delay

geometric time delay

Time delay with 1.5% accuracy

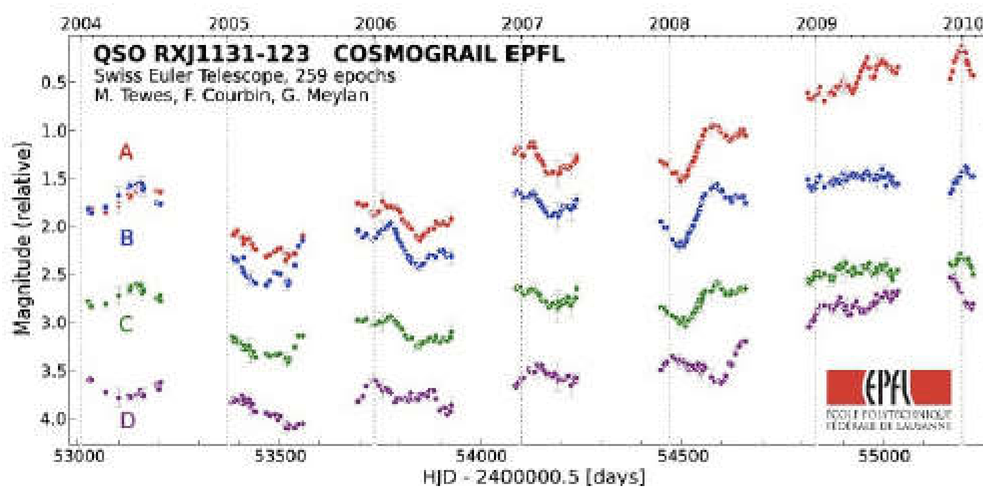

Results: Suyu et al. 2013

$$H_0 = 75.2^{+4.4}_{-4.2}\ km\ s^{-1}\ Mpc^{-1}$$

$$\Omega_{de} = 0.76^{+0.02}_{-0.03} \qquad w = -1.14^{+0.17}_{-0.20}$$

Modern cosmology: Incremental Exploration of the Unknown

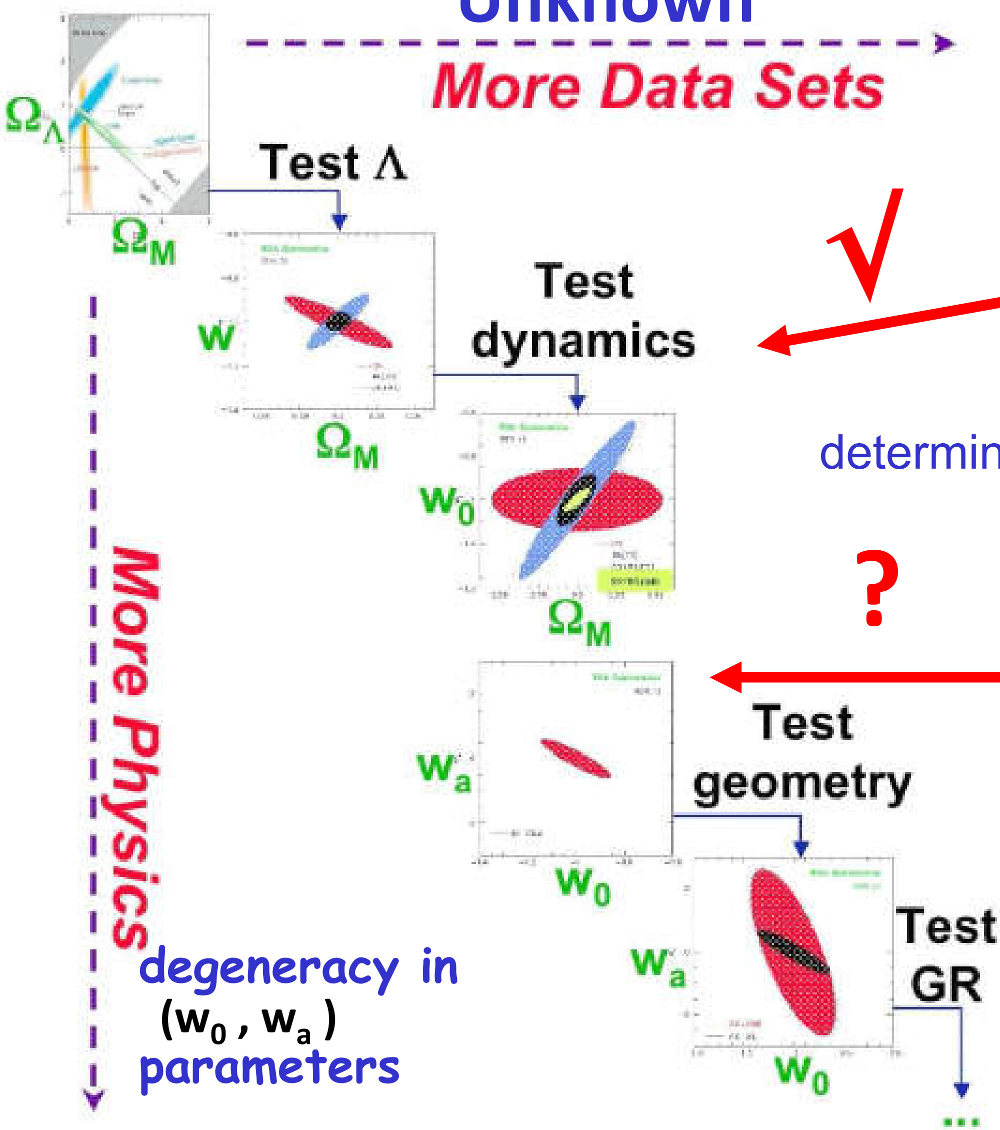

degeneracy in
(w_0 , w_a)
parameters

Linder (astro-ph/0511197)

√

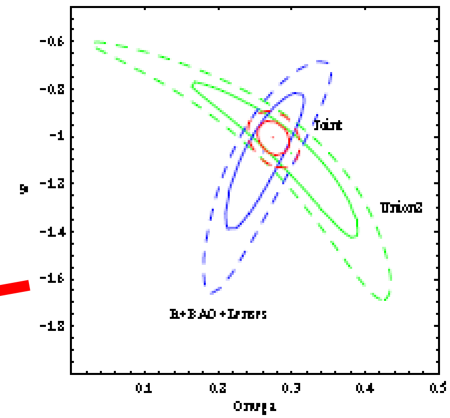

MB, B.Malec, A.Piórkowska 2011

determine cosmic equation of state $p_X = w\rho_X$

?

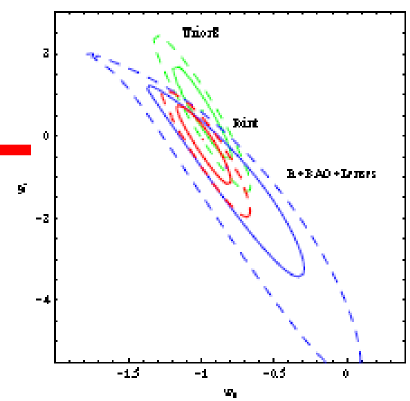

check if it evolves in time

$$w(z) = w_0 + w_a \frac{z}{1+z}$$

we need complementary tests
* break degeneracy
* coherence test

Heuristic arguments behind old searches for strong lenses: (Kochanek 2004)

- Typical galaxy with Einstein radius ϑ_E has cross section $\pi\vartheta_E^2$

- if you examine N such galaxies for a sign of lensing, you expect to find $N\,\pi\vartheta_E^2\,\Sigma_{source}$ lenses, where Σ_{source} is surface density of sources

- if you examine N sources for a galaxy in front of them, you expect to find $N\,\pi\vartheta_E^2\,\Sigma_{lens}$ lenses, where Σ_{lens} is surface density of lensing galaxies

- now, surface density of massive galaxies is much higher than surface density of easily detectable high z sources $\Sigma_{lens} \gg \Sigma_{source}$

- hence you need to examine fewer sources than galaxies to find the same number of lenses

But in the era of massive galaxy surveys (like SDSS) …

Sloan Lens ACS (SLACS) Survey

SELECTION OF LENS CANDIDATES:

- 150,000 Luminous Red +MAIN Galaxies from SDSS
  (e.g. Eisenstein et al. 2004)
- Each galaxy has a SDSS spectrum → redshift(s) & velocity dispersion
- Some spectra show higher-z emission lines.
  At least 3 emission lines including OII-$\lambda\lambda$3728 ? → **New lens?**
- HST-ACS 7-min snapshots/1 GO orbit in F435W/F555W and F814W.

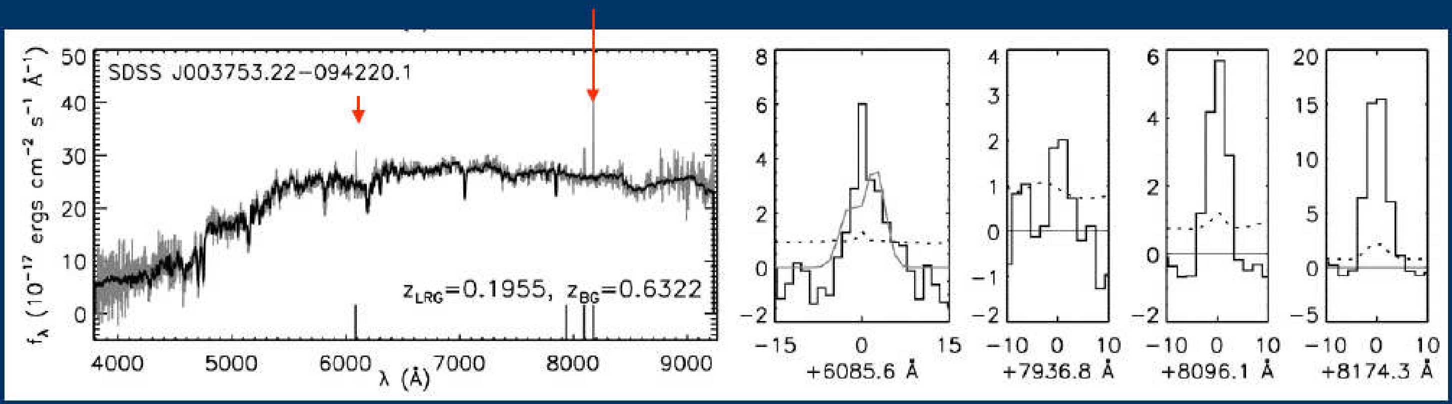

After L. Koopmans : *www.angles.eu.org/meetings/mid_term/copenhagen_leon.pdf*

Example: SDSS J2321-0939

HST + IFU Follow-up (Gemini/Magellan & VLT)

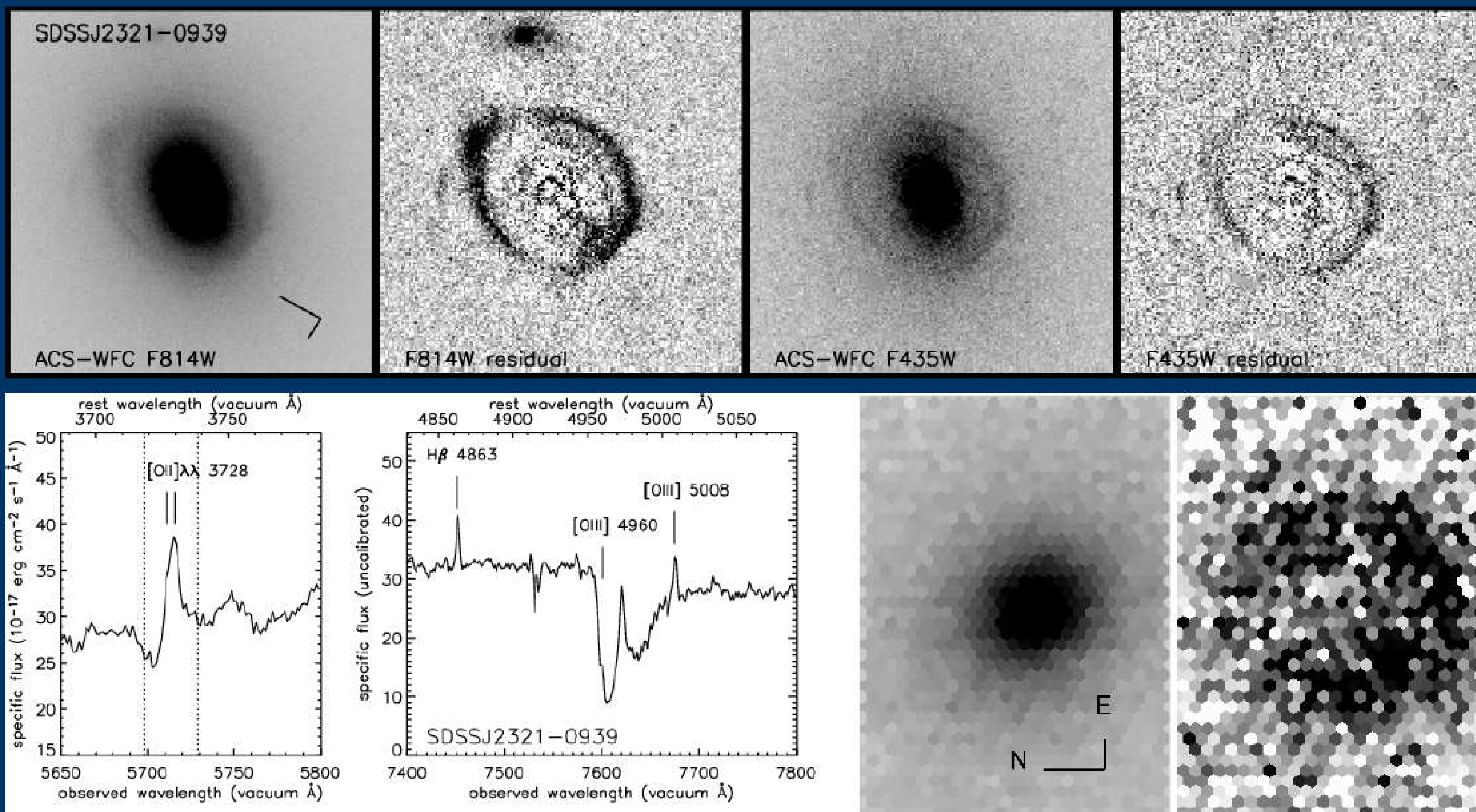

(Bolton et al. 2006)

After L. Koopmans : *www.angles.eu.org/meetings/mid_term/copenhagen_leon.pdf*

Massive spectroscopic surveys: SLACS, BELLS, SL2S SDSS, BOSS ... SL2S (CFHT)

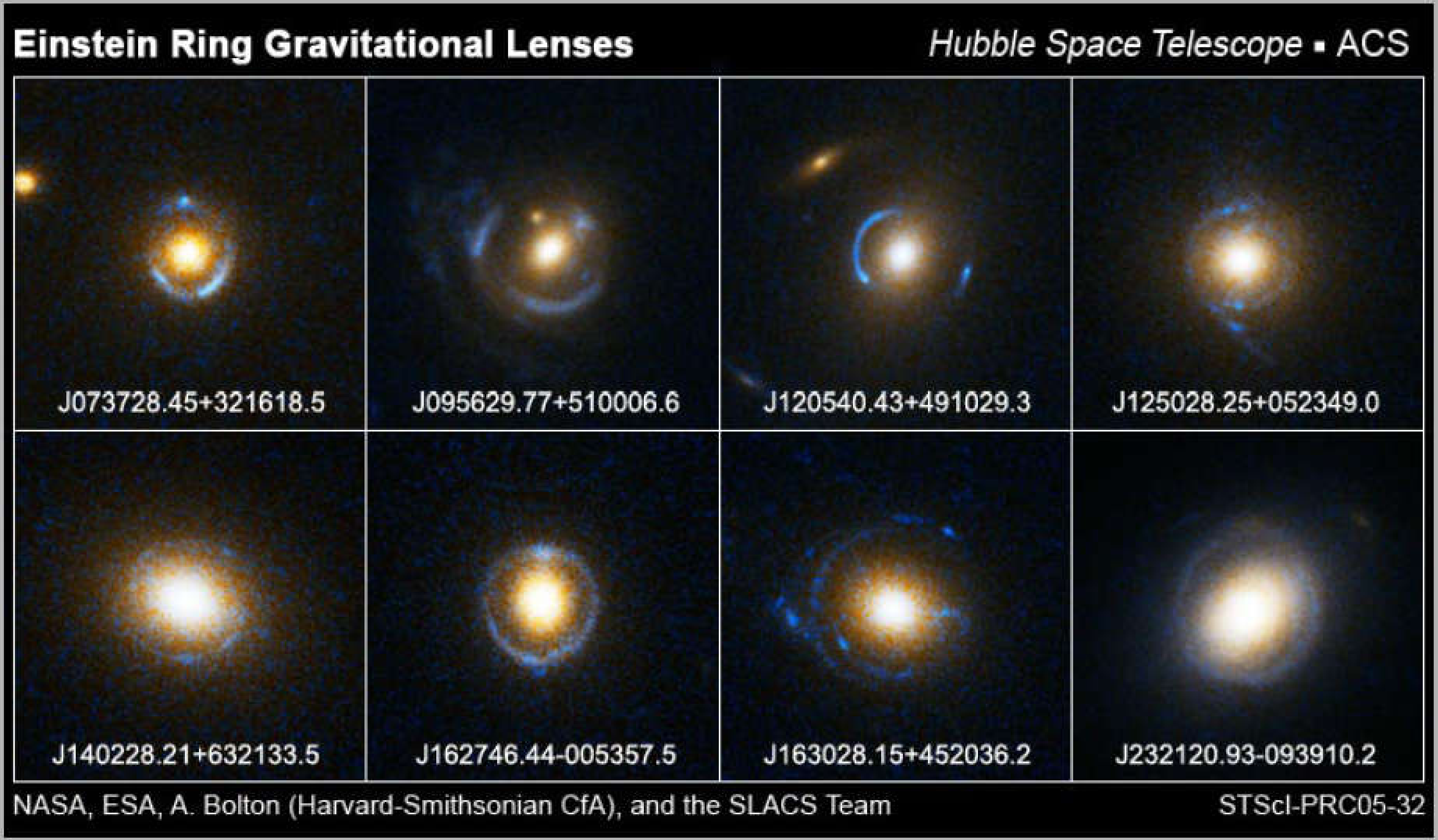

Combining Lensing & Dynamics:

GRAVITATIONAL LENSING

STELLAR DYNAMICS

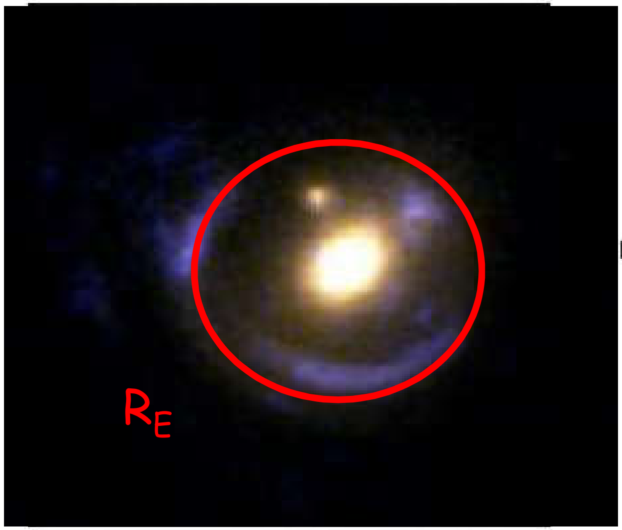

+

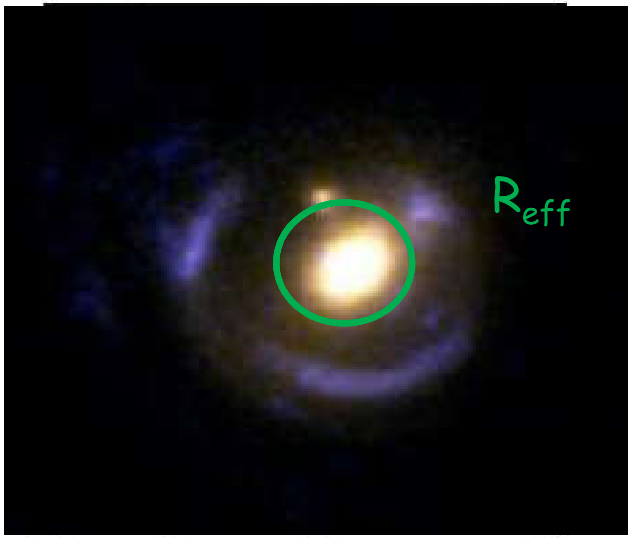

Accurate determination of total mass inside Einstein radius (projected along R_{Ein} cylinder)

Information on 3D mass profile within the region probed by kinematic observations

The density slope of E/S0 galaxies between z=0.08-0.33

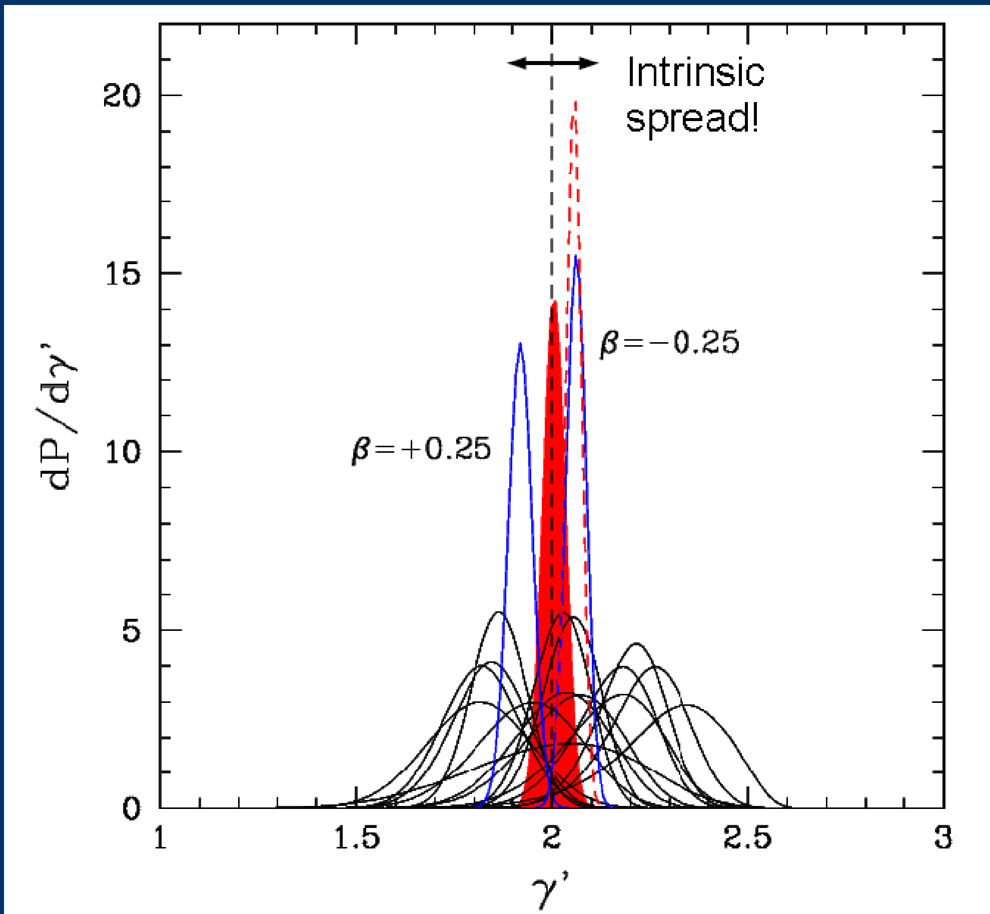

(Koopmans et al. 2006)

Total density slope inside ~0.3-1.0 R_{eff}

$\langle \gamma' \rangle = 2.01 \pm 0.03$

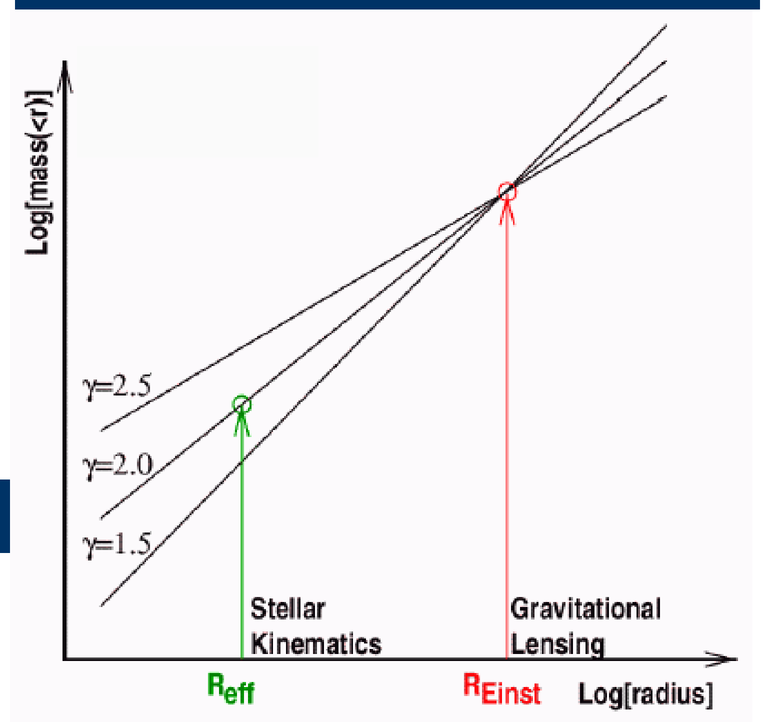

After L. Koopmans :

www.angles.eu.org/meetings/mid_term/copenhagen_leon.pdf

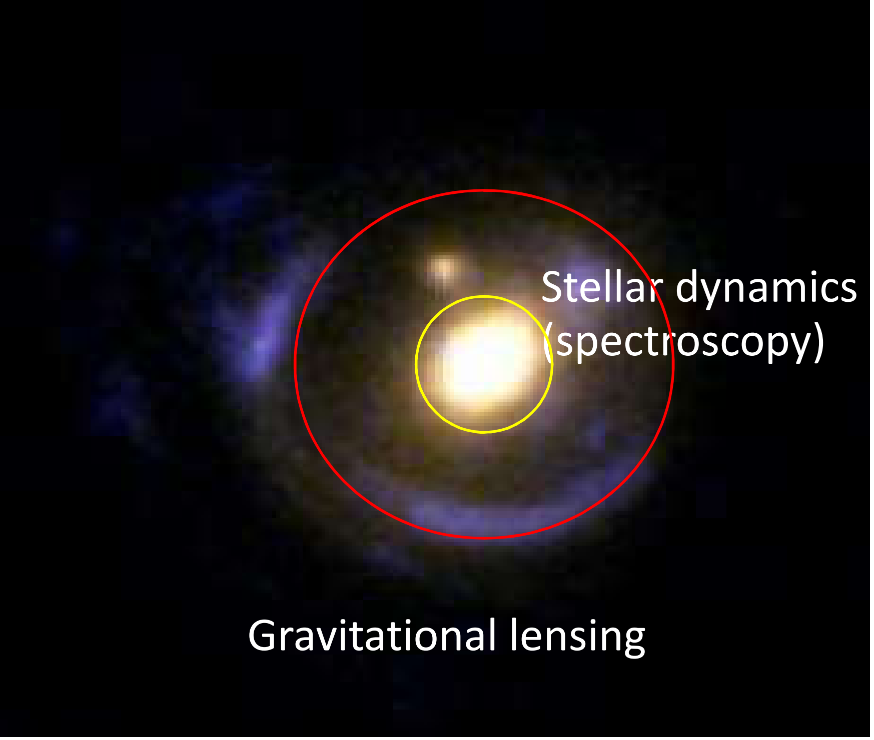

Idea

Velocity dispersion - spectroscopy

$$\theta_E = 4\pi \left(\frac{\sigma_v}{c} \right)^2 \frac{D_{LS}}{D_S}$$

From angular separation of images

Ratio determined by cosmological model

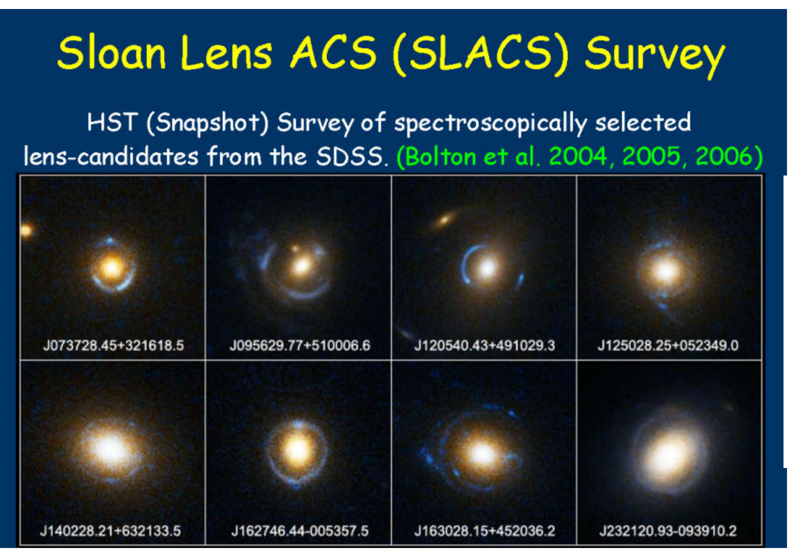

Monthly Notices of the ROYAL ASTRONOMICAL SOCIETY

Mon. Not. R. Astron. Soc. **406,** 1055–1059 (2010) doi:10.1111/j.1365-2966.2010.16725.x

Cosmic equation of state from strong gravitational lensing systems

Marek Biesiada,★ Aleksandra Piórkowska★ and Beata Malec★

Department of Astrophysics and Cosmology, Institute of Physics, University of Silesia, Uniwersytecka 4, 40-007 Katowice, Poland

Journal of Cosmology and Astroparticle Physics
An IOP and SISSA journal

Constraints on cosmological models from strong gravitational lensing systems

Shuo Cao,[a] Yu Pan,[a,b] Marek Biesiada,[c] Wlodzimierz Godlowski[d] and Zong-Hong Zhu[a,1]

JCAP03(2012)016

10 cluster lenses
70 galaxy lenses
from SLACS

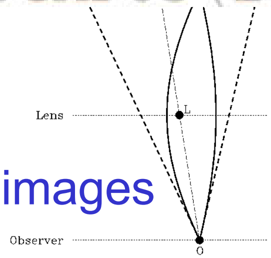

2 images

$$\theta_E = 4\pi \frac{\sigma_{SIS}^2}{c^2} \frac{D_{ls}}{D_s}$$

$$\mathcal{D}^{obs} = \frac{c^2 \theta_E}{4\pi \sigma_0^2 f_E^2}$$

Subsample
of 2 image systems

36 SLACS lenses

$$\sigma_{SIS} = f_E \sigma_0$$

marginalize over $\mathbf{f_E}$

$$\mathcal{L}(\mathrm{p}) = \int \mathcal{L}(\mathrm{p}, f_E) P(f_E) df_E$$

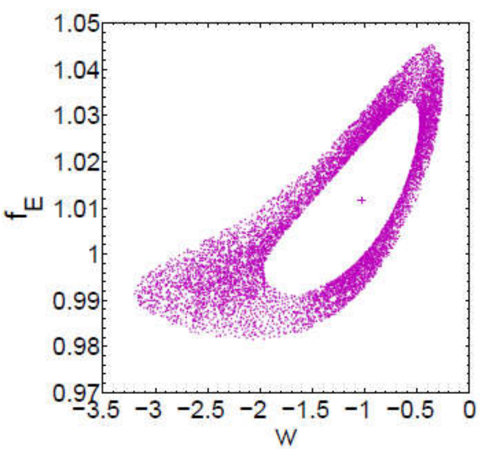

2 image sample

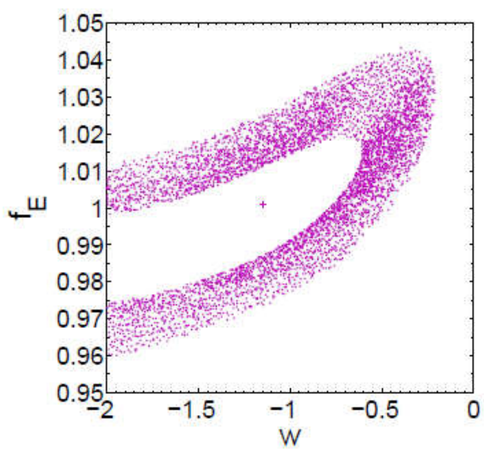

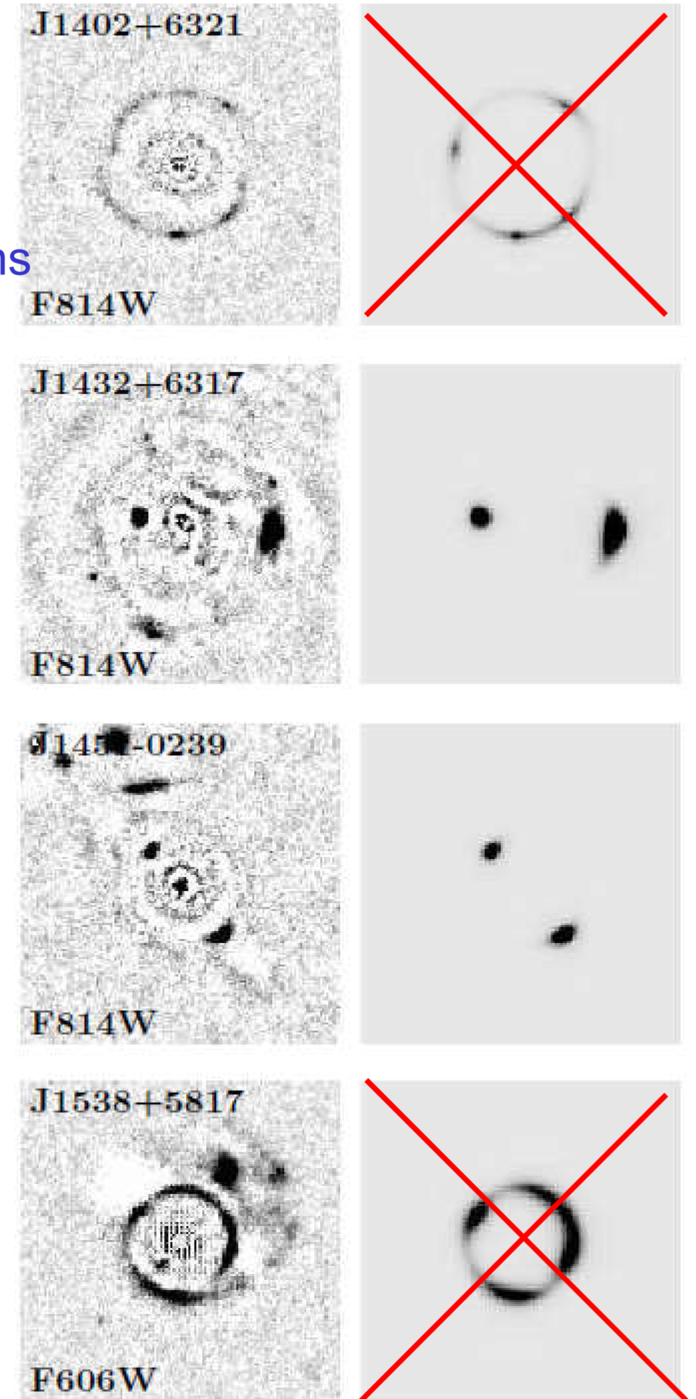

cluster + galaxy strong lenses

Cosmological model	Best-fitting parameters ($n = 80$)	Best-fitting parameters ($n = 46$)
ΛCDM	$\Omega_m = 0.20^{+0.07}_{-0.07}$	$\Omega_m = 0.26^{+0.11}_{-0.10}$
wCDM	$w = -1.02^{+0.26}_{-0.26}$	$w = -1.15^{+0.34}_{-0.35}$
CPL	$w_0 = 0.60 \pm 1.76$	$w_0 = -0.24 \pm 2.42$
	$w_a = -7.37 \pm 8.05$	$w_a = -6.35 \pm 9.75$

Present values

WMAP7+BAO+H

$\Omega_m = 0.272$

$w = -1.10 \pm 0.14$

$w_0 = -0.93 \pm 0.13$

$w_a = -0.41 \pm 0.71$

Komatsu et al. 2011

Full sample

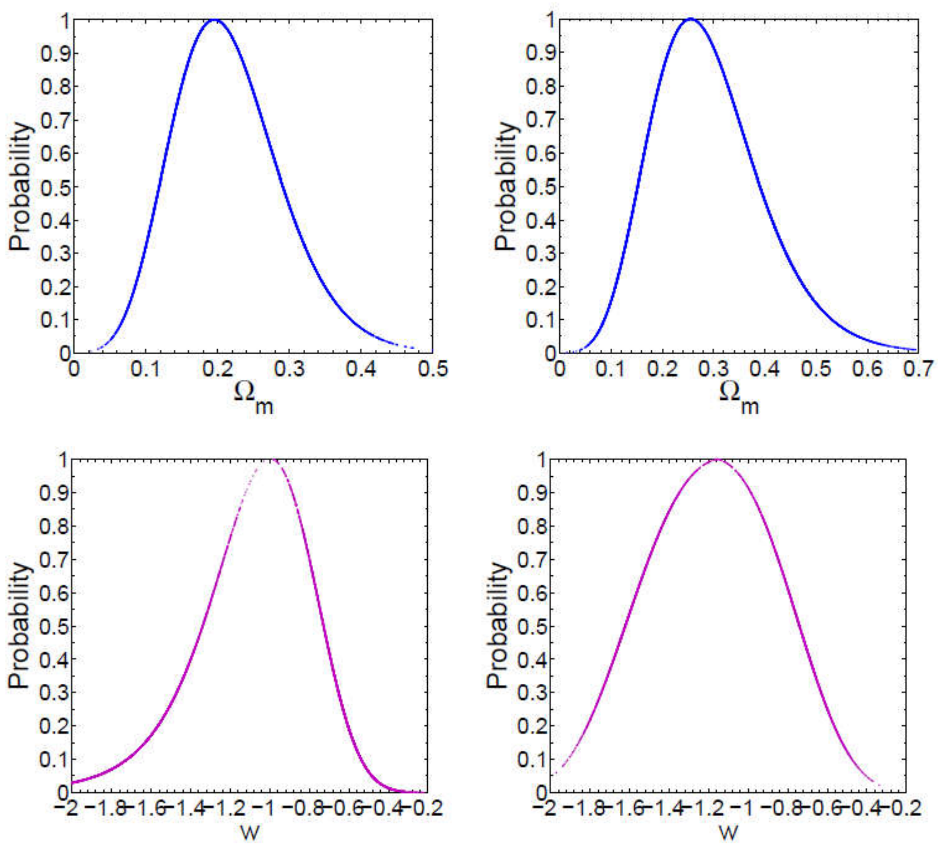

2 image lens sample

THE ASTROPHYSICAL JOURNAL, 806:185 (12pp), 2015 June 20
doi:10.1088/0004-637X/806/2/185

COSMOLOGY WITH STRONG-LENSING SYSTEMS

SHUO CAO[1], MAREK BIESIADA[1,2], RAPHAËL GAVAZZI[3], ALEKSANDRA PIÓRKOWSKA[2], AND ZONG-HONG ZHU[1]
[1] Department of Astronomy, Beijing Normal University, Beijing 100875, China; zhuzh@bnu.edu.cn
[2] Department of Astrophysics and Cosmology, Institute of Physics, University of Silesia, Uniwersytecka 4, 40-007, Katowice, Poland
[3] Institute d'Astrophysique de Paris, UMR7095 CNRS—Universite Pierre et Marie Curie, 98bis bd Arago, F-75014 Paris, France
Received 2015 January 23; accepted 2015 May 1; published 2015 June 17

Spherical power-law mass distribution

$$\rho \propto r^{-\gamma}$$

Stellar dynamics (spherical Jeans equation): mass inside projected aperture radius scaled to Einstein radius

Lensing: mass inside Einstein radius

$$M_{\rm lens} = \frac{c^2}{4G}\frac{D_s D_l}{D_{ls}}\theta_E^2$$

+

$$M_{\rm dyn} = \frac{\pi}{G}\sigma_{ap}^2 R_E \left(\frac{R_E}{R_{ap}}\right)^{2-\gamma} f(\gamma)$$

$$= \frac{\pi}{G}\sigma_{ap}^2 D_l \theta_E \left(\frac{\theta_E}{\theta_{ap}}\right)^{2-\gamma} f(\gamma)$$

$$\theta_E = 4\pi \frac{\sigma_{ap}^2}{c^2}\frac{D_{ls}}{D_s}\left(\frac{\theta_E}{\theta_{ap}}\right)^{2-\gamma} f(\gamma)$$

Based on SLACS
Koopmans et al. 2006

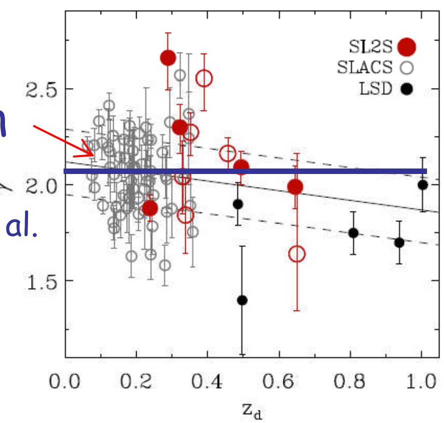

A.Ruff , R.Gavazzi et al. 2010

$$\gamma(z_l) = \gamma_0 + \gamma_1 z_l$$

γ slope evolution

$$D^{\rm obs} = \frac{c^2\theta_E}{4\pi\sigma_{ap}^2}\left(\frac{\theta_{ap}}{\theta_E}\right)^{2-\gamma} f^{-1}(\gamma)$$

vs.

$$D^{\rm th}(z_l, z_s; p) = \frac{D_{ls}(p)}{D_s(p)} = \frac{\int_{z_l}^{z_s} \frac{dz'}{h(z';p)}}{\int_0^{z_s} \frac{dz'}{h(z';p)}}$$

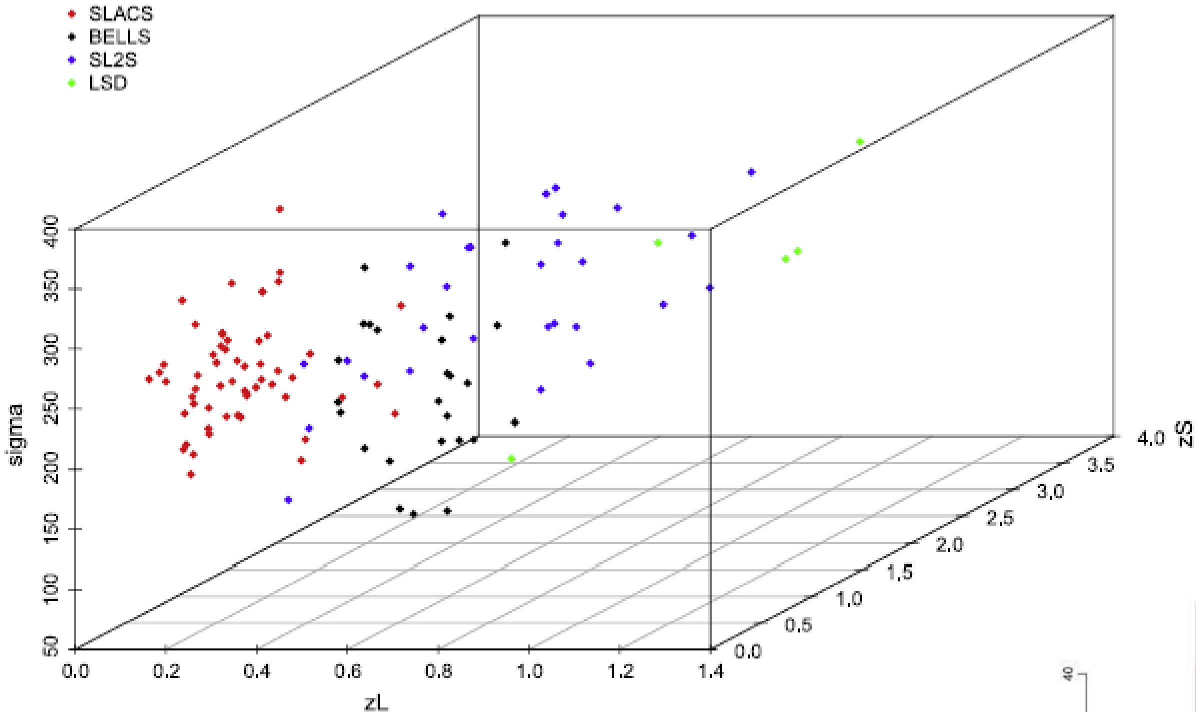

118 lenses:

SLACS	57
BELLS	25
SL2S	5
LSD	5

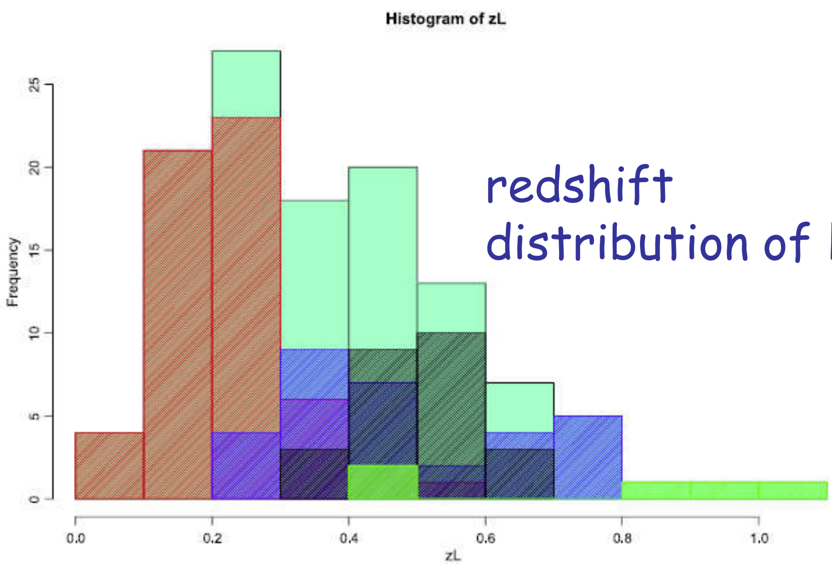

redshift
distribution of lenses

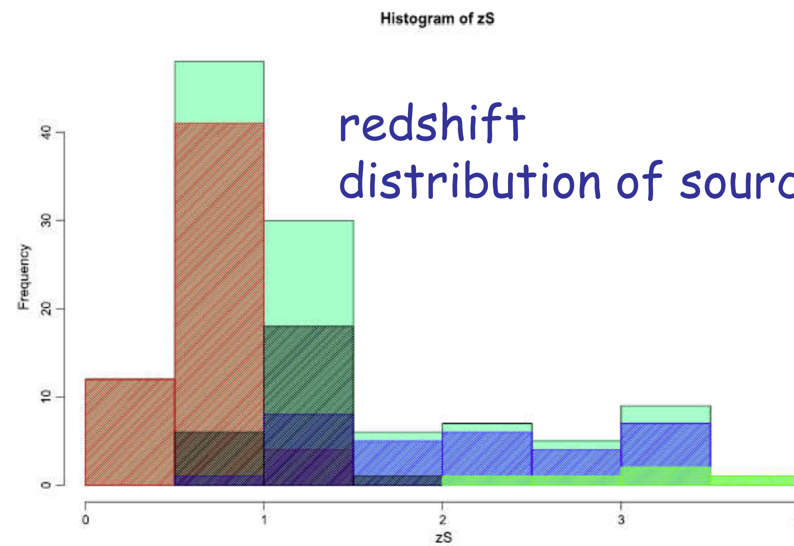

redshift
distribution of sources

THE ASTROPHYSICAL JOURNAL, 806:185 (12pp), 2015 June 20 CAO ET AL.

Table 2
Dark Energy (XCDM Model and CPL Parametrization) Constraints Obtained on the Full 118 Strong-lensing (SL) Sample[a]

Cosmology (Sample)	w_0	w_1	γ_0	γ_1
XCDM1 (SL; σ_{ap})	$w_0 = -1.45^{+0.54}_{-0.95}$	$w_1 = 0$	$\gamma_0 = 2.03 \pm 0.06$	$\gamma_1 = 0$
XCDM1 (SL; σ_0)	$w_0 = -1.15^{+0.56}_{-1.20}$	$w_1 = 0$	$\gamma_0 = 2.07 \pm 0.07$	$\gamma_1 = 0$
XCDM2 (SL; σ_{ap})	$w_0 = -1.48^{+0.54}_{-0.94}$	$w_1 = 0$	$\gamma_0 = 2.06 \pm 0.09$	$\gamma_1 = -0.09 \pm 0.16$
XCDM2 (SL; σ_0)	$w_0 = -1.35^{+0.67}_{-1.50}$	$w_1 = 0$	$\gamma_0 = 2.13^{+0.07}_{-0.12}$	$\gamma_1 = -0.09 \pm 0.17$
CPL1 (SL; σ_{ap})	$w_0 = -0.15^{+1.27}_{-1.60}$	$w_1 = -6.95^{+7.25}_{-3.05}$	$\gamma_0 = 2.08 \pm 0.09$	$\gamma_1 = -0.09 \pm 0.17$
CPL1 (SL; σ_0)	$w_0 = -1.00^{+1.54}_{-1.95}$	$w_1 = -1.85^{+4.85}_{-6.75}$	$\gamma_0 = 2.14^{+0.07}_{-0.10}$	$\gamma_1 = -0.10 \pm 0.18$
CPL2 (SL; σ_{ap})	$w_0 = -0.16^{+1.21}_{-1.48}$	$w_1 = -6.25^{+6.25}_{-3.75}$	$\gamma_0 = 2.08$	$\gamma_1 = -0.09$
CPL2 (SL; σ_0)	$w_0 = -1.05^{+1.43}_{-1.77}$	$w_1 = -1.65^{+4.25}_{-6.35}$	$\gamma_0 = 2.14$	$\gamma_1 = -0.10$
CPL2 (SN)	$w_0 = -1.00 \pm 0.40$	$w_1 = -0.12^{+1.58}_{-2.78}$	□	□

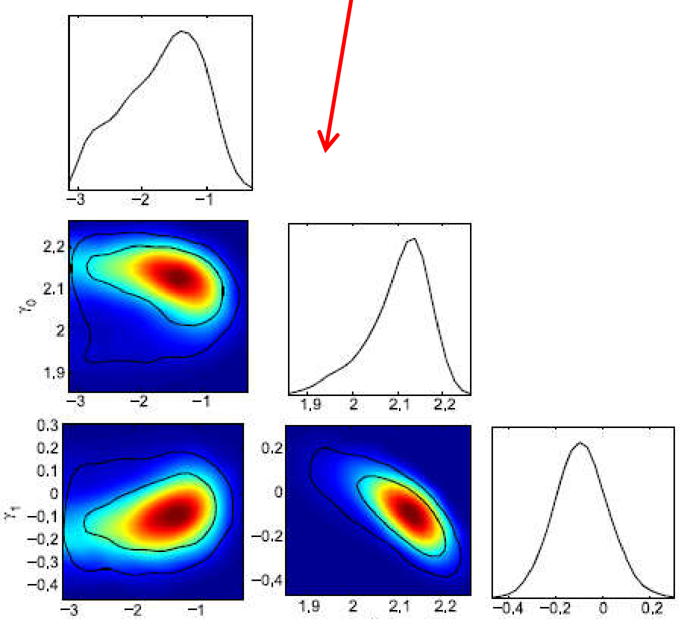

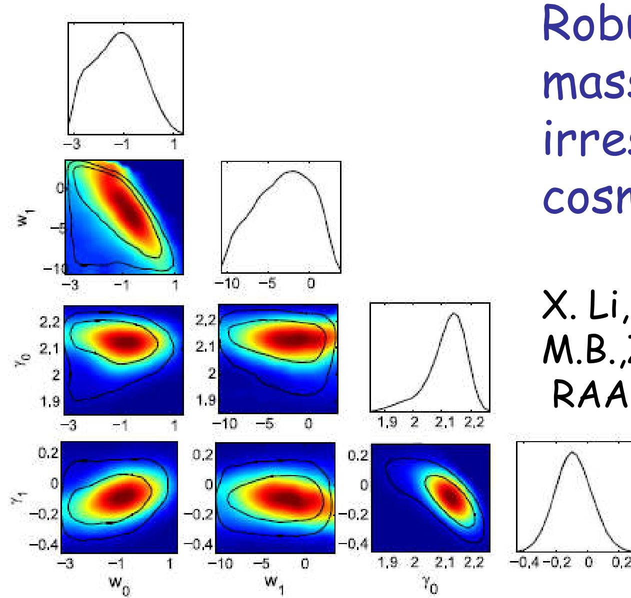

Robust inference of mass density profile – irrespective of cosmological model

X. Li, S. Cao, X.Zheng, M.B.,Z-H. Zhu
RAA, 16, 84 (2016)

THE ASTROPHYSICAL JOURNAL

THE DISTANCE DUALITY RELATION FROM STRONG GRAVITATIONAL LENSING

Kai Liao[1], Zhengxiang Li[2], Shuo Cao[2], Marek Biesiada[2,3], Xiaogang Zheng[2], and Zong-Hong Zhu[2]

Published 2016 May 10 •

The Astrophysical Journal, Volume 822, Number 2

Limits on the power-law mass and luminosity density profiles of elliptical galaxies from gravitational lensing systems

MNRAS (2016) in print

Shuo Cao[1], Marek Biesiada[1,2], Meng Yao[1], and Zong-Hong Zhu[1]⋆

[1] *Department of Astronomy, Beijing Normal University, 100875, Beijing, China;*

[2] *Department of Astrophysics and Cosmology, Institute of Physics, University of Silesia, Uniwersytecka 4, 40-007 Katowice, Poland*

Comparison of cosmological models using standard rulers and candles

RAA 16, 84 (2016)

Xiaolei Li,[1] Shuo Cao,[1] Xiaogang Zheng[1], and Marek Biesiada,[1,2]

[1] Department of Astronomy, Beijing Normal University, Beijing 100875, China;
lixiaolei@mail.bnu.edu.cn

[2] Department of Astrophysics and Cosmology, Institute of Physics, University of Silesia, Uniwersytecka 4, 40-007 Katowice, Poland

Why strong lensing systems ?

Dark Energy Complementarity

- We expect that the greatest accuracy and confidence in the measurements will come from independent crosschecks and complementarity between different methods probing the cosmology:

Albrecht et al. (DETF) 2006

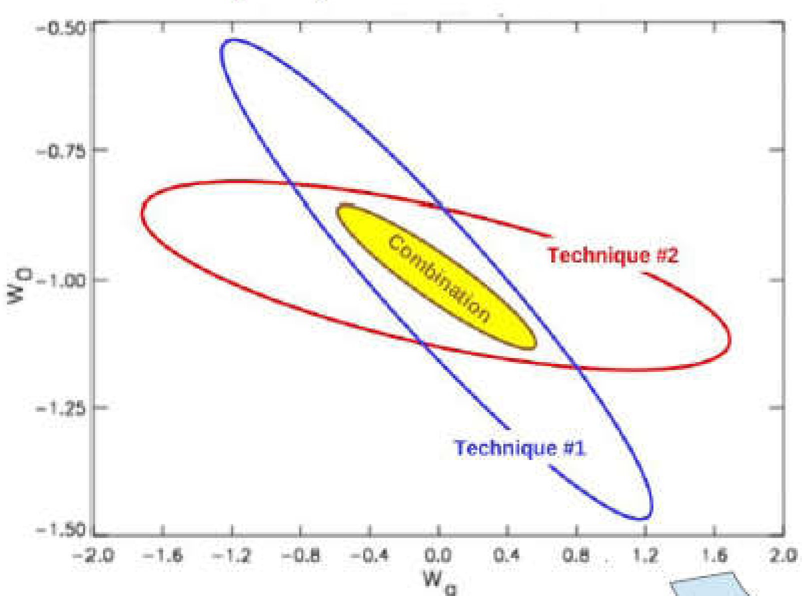

Illustration of the power of combining techniques.

Biesiada, Malec, AP, 2011

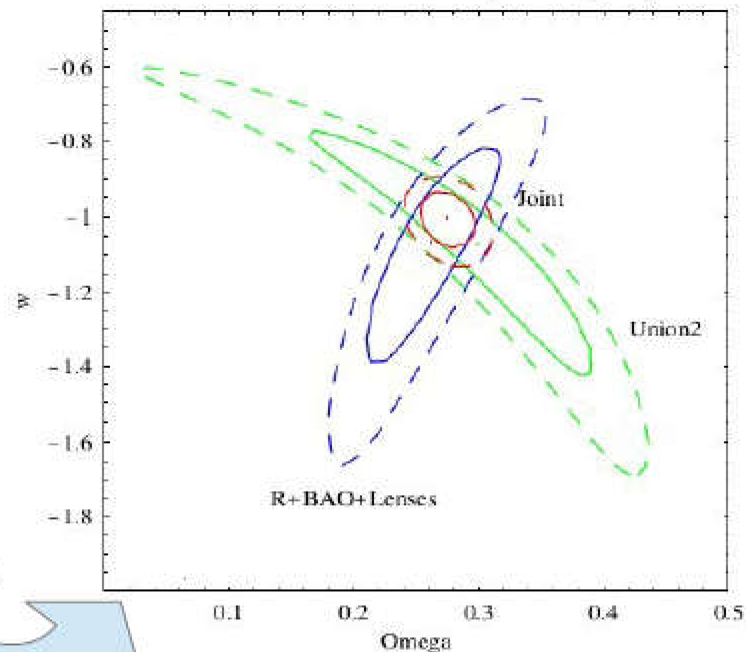

just like complementarity of standard rulers and standard candles in Omega-w parameter plane

After: A.Piórkowska http://acp15.fuw.edu.pl/talks/Piorkowska.pdf

Complementarity of strong lensing measurements

- For a certain redshift range competition between two ingredients in the distance ratios in stron gravitational lensing measurements may cause a positive correlation between w0 and wa:

$$\mathcal{D}^{\mathrm{th}}(z_{\mathrm{l}}, z_{\mathrm{s}}; \boldsymbol{p}) = \frac{D_{\mathrm{s}}(\boldsymbol{p})}{D_{\mathrm{ls}}(\boldsymbol{p})} = \frac{\int_0^{z_{\mathrm{s}}} \frac{dz'}{h(z'; \boldsymbol{p})}}{\int_{z_{\mathrm{l}}}^{z_{\mathrm{s}}} \frac{dz'}{h(z'; \boldsymbol{p})}}$$

$$\frac{\partial D^{th}}{\partial p_i}$$

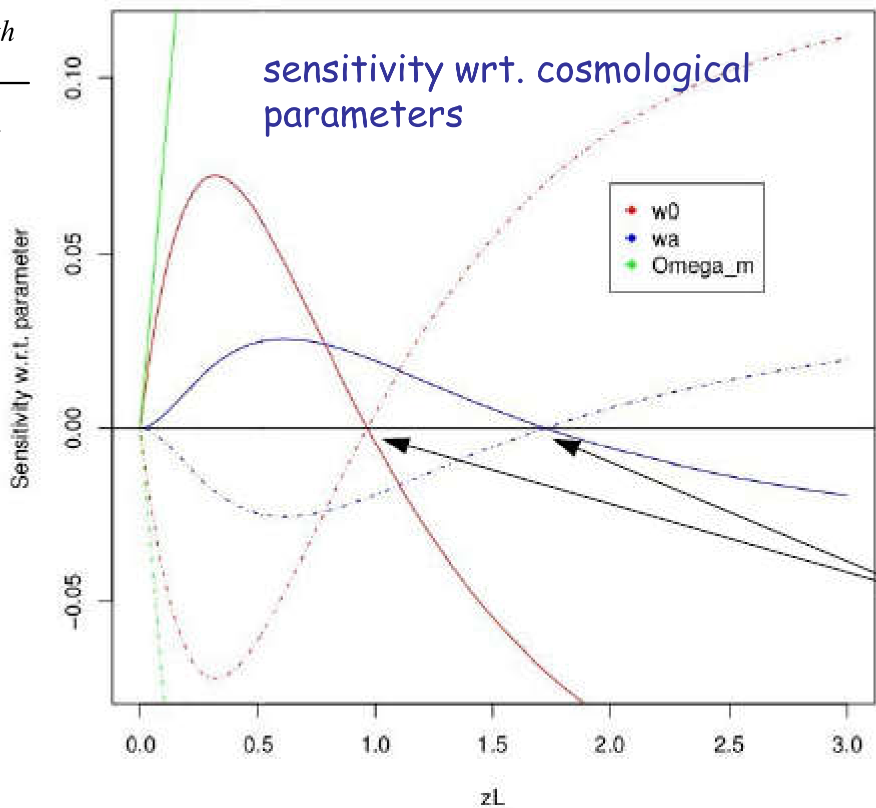

we expect that the correlation between w0 and wa should shift from negative to positive depending on the redshift

the crossings from negative to positive sensitivity occur at different redshifts

We consider here only: $z_s = 2z_l$

After: A.Piórkowska http://acp15.fuw.edu.pl/talks/Piorkowska.pdf

Complementarity of strong lensing measurements

- Strong lensing measurements are not perfect orthogonal to other distance measurement methods in the w0-wa plane but to a certain extent they can be considered as complementary:

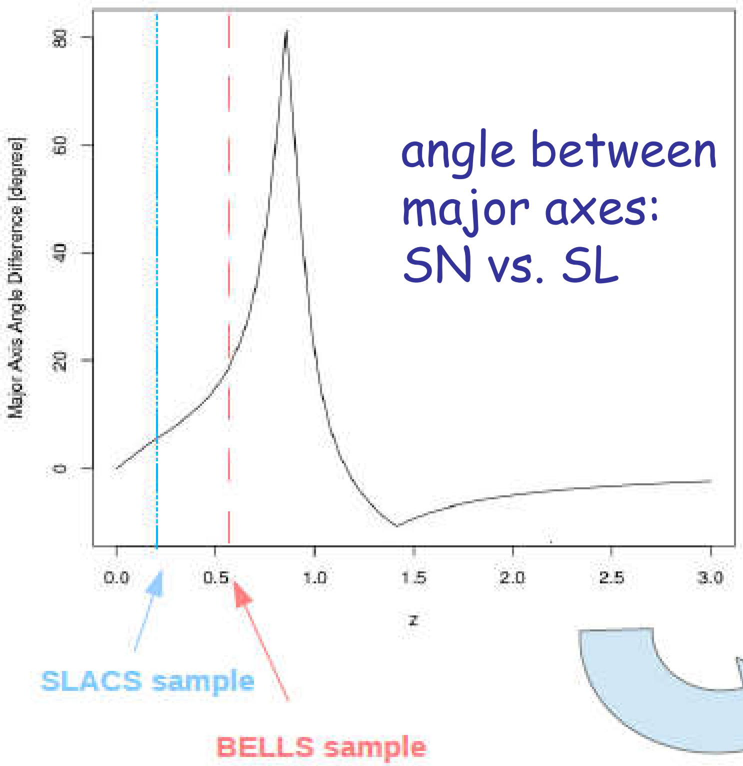

major axis angle of confidence contour for an idealized experiment as a function of redshift:

confidence contours for an idealized experiment measuring the distance ratio for several samples with different redshifts:

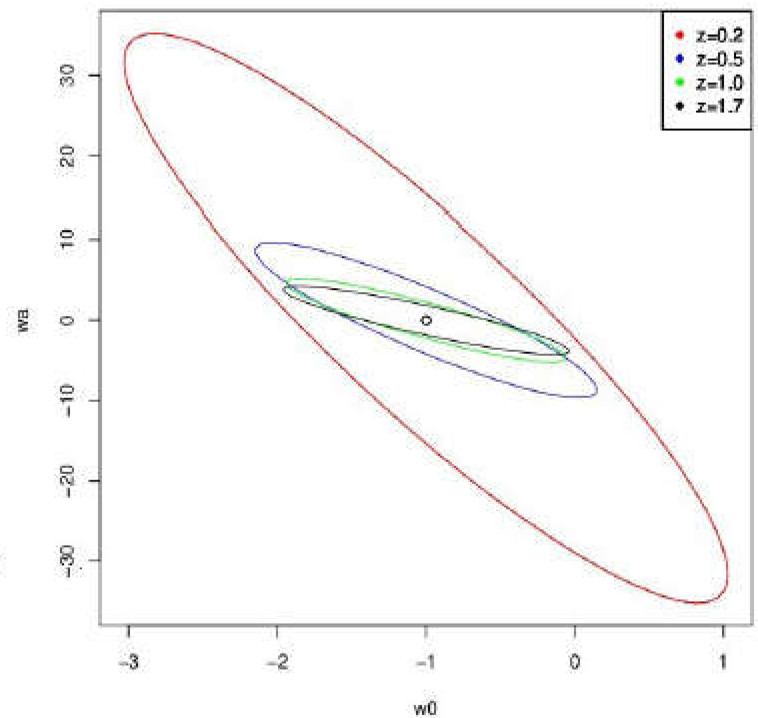

AP, Biesiada & Gavazzi, 2013

After: A.Piórkowska http://acp15.fuw.edu.pl/talks/Piorkowska.pdf

Two Einstein ring systems

If strong lensing provides M_{Einst} accurately inside R_{Einst}, then having two rings provides the density profile inside the two rings w/o hardly any assumption.

Color Composite

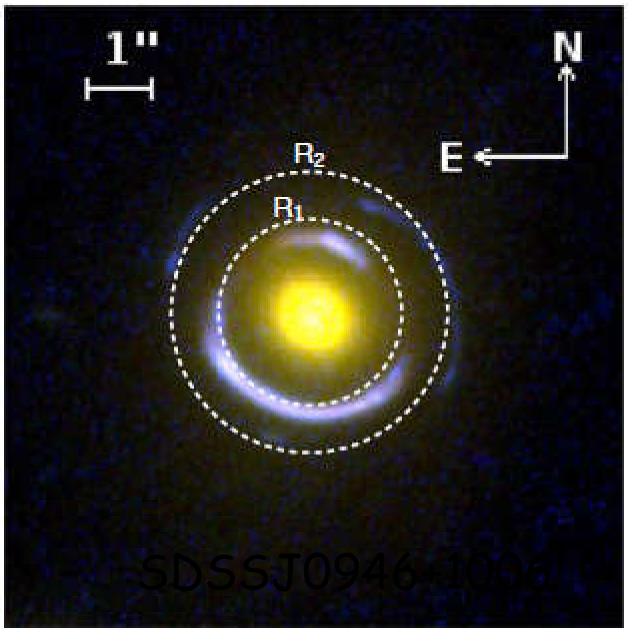

Multi-color HST data

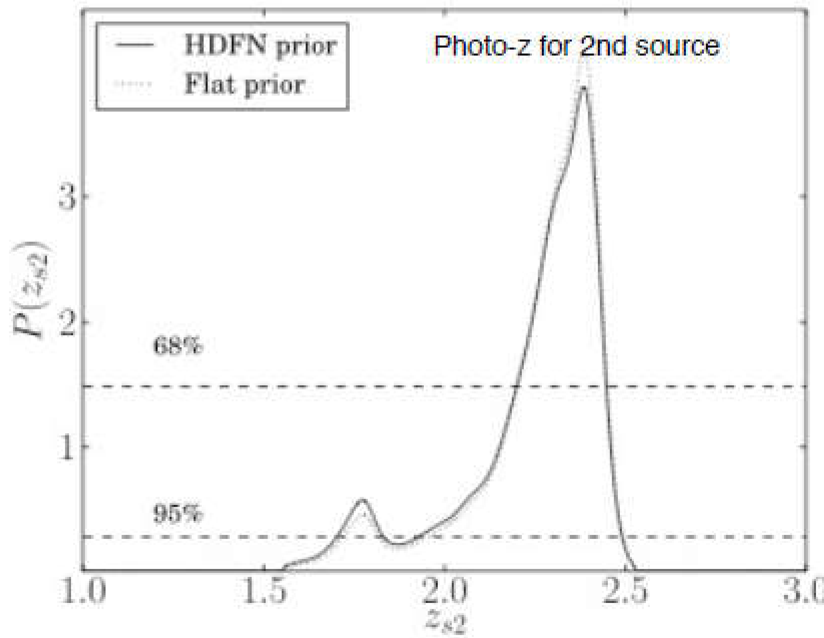

Sonnenfeld et al. 2012

Gavazzi R., Treu T., Koopmans L. V. E., Bolton A. S., Moustakas L. A., Burles S., Marshall P. J., 2008, ApJ, 677, 1046

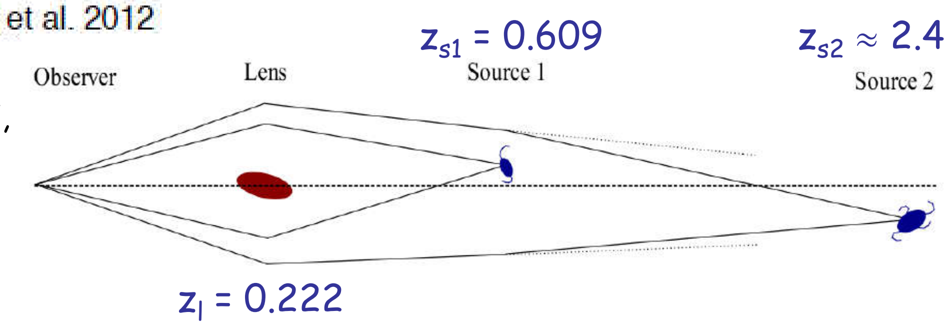

Constraining the dark energy equation of state with double source plane strong lenses

MNRAS 432, 679 (2013)

T. E. Collett[1*], M. W. Auger[1], V. Belokurov[1], P. J. Marshall[2] and A. C. Hall[1,3]
[1] Institute of Astronomy, University of Cambridge, Madingley Road, Cambridge CB3 0HA
[2] Department of Physics, University of Oxford, Keble Road, Oxford, OX1 3RH
[3] Kavli Institute for Cosmology, University of Cambridge Madingley Road, Cambridge CB3 0HA

The observable:

The Ratio of Einstein Radii.

$$\eta = \frac{\theta_{E,1}}{\theta_{E,2}}$$

$$\theta_E^{SIS} = 4\pi \frac{\sigma_V^2}{c^2} \frac{D_{ls}}{D_s}$$

$$\eta^{SIS} = \frac{D_{ls1} D_{s2}}{D_{ls2} D_{s1}}$$

No dependence on the Hubble constant!

Doubling Strong Lensing as a Cosmological Probe

Eric V. Linder
Berkeley Center for Cosmological Physics & Berkeley Lab,
University of California, Berkeley, CA 94720, USA
(Dated: May 18, 2016)

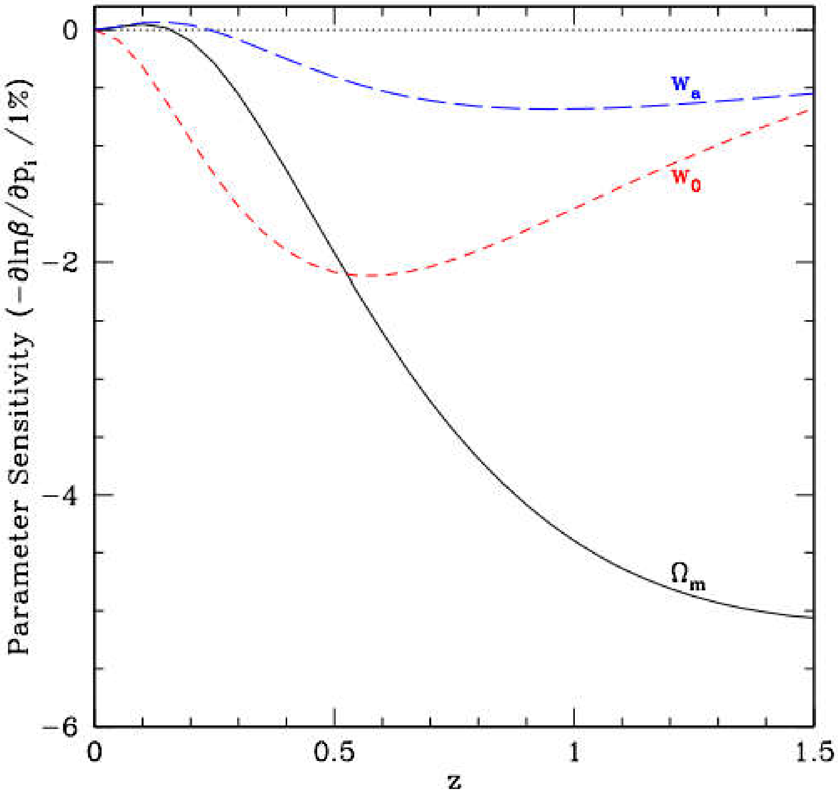

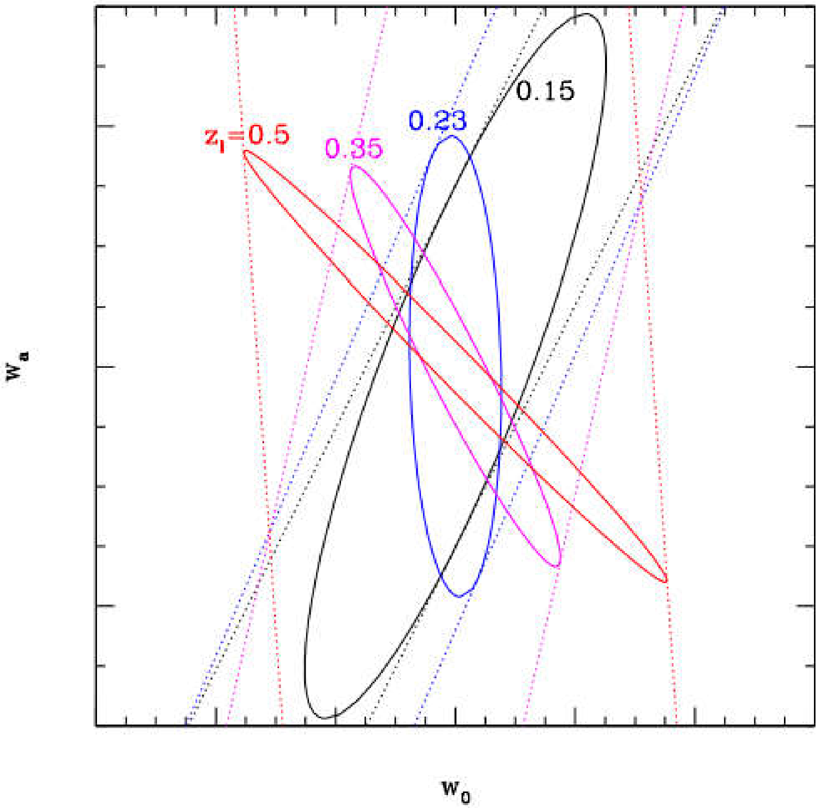

arXiv:1605.04910v1 [astro-ph.CO]

THE POPULATION OF GALAXY-GALAXY STRONG LENSES IN FORTHCOMING OPTICAL IMAGING SURVEYS

THOMAS E. COLLETT
Institute of Cosmology and Gravitation, University of Portsmouth, Burnaby Rd, Portsmouth, PO1 3FX, UK
Submitted to the Astrophysical Journal, 2015 May 28

ABSTRACT

Ongoing and future imaging surveys represent significant improvements in depth, area and seeing compared to current data-sets. These improvements offer the opportunity to discover up to three orders of magnitude more galaxy-galaxy strong lenses than are currently known. In this work we forecast the number of lenses discoverable in forthcoming surveys and simulate their properties. We generate a population of statistically realistic strong lenses and simulate observations of this population for the Dark Energy Survey (DES), Large Synoptic Survey Telescope (LSST) and Euclid surveys. We verify our model against the galaxy-scale lens search of the Canada-France-Hawaii Telescope Legacy Survey (CFHTLS), predicting 250 discoverable lenses compared to 220 found by Gavazzi et al. (2014). The predicted Einstein radius distribution is also remarkably similar to that found by Sonnenfeld et al. (2013). For future surveys we find that, assuming Poisson limited lens galaxy subtraction, searches in DES, LSST and Euclid datasets should discover 2400, 120000, and 170000 galaxy-galaxy strong lenses respectively. Finders using blue minus red $(g - i)$ difference imaging for lens subtraction can discover 1300 and 62000 lenses in DES and LSST. The uncertainties on the model are dominated by the high redshift source population which typically gives fractional errors on the discoverable lens number at the tens of percent level. We find that doubling the signal-to-noise ratio required for a lens to be detectable, approximately halves the number of detectable lenses in each survey, indicating the importance of understanding the selection function and sensitivity of future lens finders in interpreting strong lens statistics. We make our population forecasting and simulated observation codes publicly available so that the selection function of strong lens finders can easily be calibrated.

Perspectives for strong lensing:

* increasing number of strong lenses discovered by searches such as CLASS , SLACS, SL2S, SQLS, HAGGLeS, AEGIS, COSMOS, CASSOWARY, BELLS

* new projects: Pan-STARRS, LSST, JDEM / IDECS3, SKA4 will yield an explosion in the number of strong lenses

- strongly lensed systems with known central velocity dispersions are a new class of "standard rulers" (Einstein radius being standardized by stellar kinematics)

- their use entered the stage of providing first estimates on cosmological parameters

- they will develop into a technique complementary to other methods


DZIĘKUJĘ ZA UWAGĘ !
Thank you !